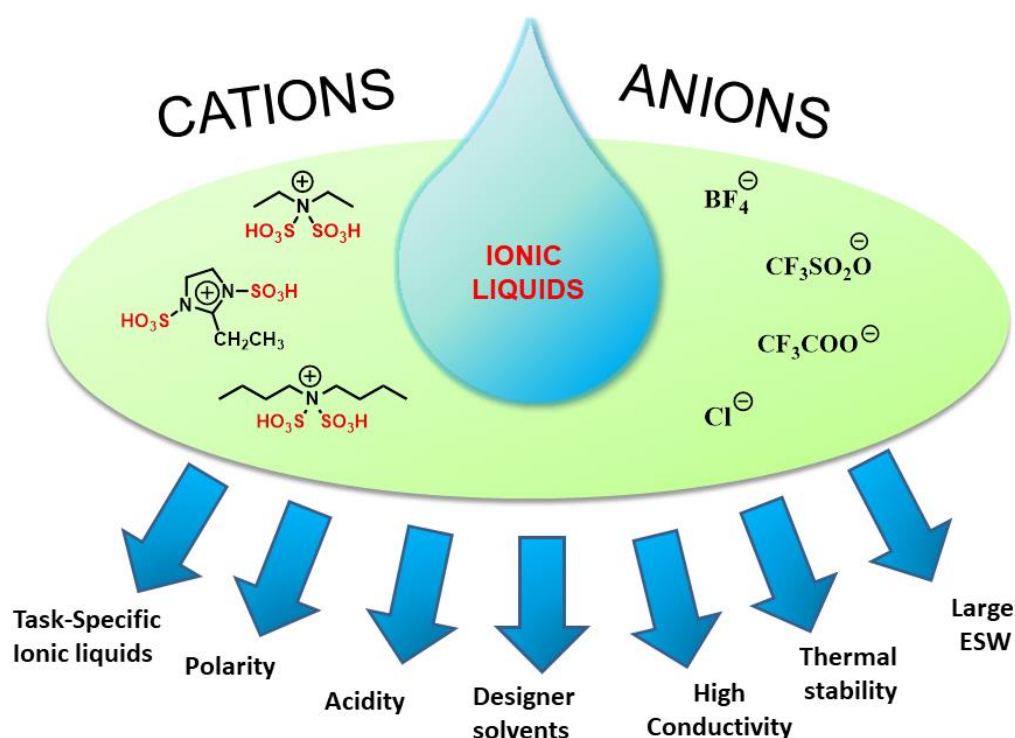


Chapter 4

Comparative Study on the Physicochemical Properties of N-SO₃H Functionalized Ammonium and Imidazolium Based Brønsted Acidic Ionic Liquids



4.1 Introduction

In section 3.1 of Chapter 3, it was mentioned that over the last few decades several research articles have been published on the synthesis of task-specific room temperature ILs with diverse physicochemical properties which include ionic conductivities, viscosity, electrochemical stability window (ESW), thermal stability, acidity, density, moisture sensitivity etc. [1-24]. These articles also provide in depth information regarding their potential uses as catalyst, reaction medium, electrolytes in battery, sensors, separation media and fuel-cell, electrophoresis media and so on [16-24]. Some of these research articles were solely focussed on the $-\text{SO}_3\text{H}$ group functionalized ionic liquids based on imidazolium, ammonium, pyridinium and phosphonium cations [1, 14, 15, 23-28].

Known as the designer solvents, the physicochemical properties of these ILs can be easily tuned by varying the combination of its constituent ions. Selecting an appropriate cation-anion pair can lead to the formation of ILs with large ionic conductivities, broader electrochemical windows, high thermal stability, and lower viscosities [20, 29, 30]. Such properties make the ILs desirable candidates for application in electrochemical devices and fuel cells. The Electrochemical Stability Windows (ESWs) of some common ILs are found in the range of 4.5-5 V and which is larger than that of aqueous electrolytes [31]. Although, the synthesis of RTILs with lower viscosities and high electrochemical stabilities and ionic conductivities is still difficult.

It has been found that the quaternary ammonium ILs display higher redox stability compared to the imidazolium ILs [18, 32]. However, their high viscosity limits their electrochemical applications. Switching the ammonium cation with the imidazolium cation allows us to obtain ILs with lower viscosities and thus, higher ionic conductivities [29, 31]. The chain length of alkyl substituents in the ILs is also an important factor affecting their ESWs, conductivities, densities, viscosities, acidity etc. [33].

For electrochemical applications of RTILs, all these above-mentioned limitations can be reduced by mixing them with various molecular solvents. These binary mixtures involve different solvent-ion interactions [17, 34-36]. Several research articles display the physicochemical behaviour of the available ammonium and imidazolium based RTILs and their binary mixtures with molecular solvents. Buzzeo et al. compared the electrochemical stability windows of various alkylated ammonium, imidazolium and phosphonium ionic liquids in acetonitrile [35]. It was found that the phosphonium ILs in

acetonitrile displayed wider ESWs followed by the ammonium ILs and then the imidazolium ILs. The presence of water as an impurity also influenced the electrochemical stability of imidazolium ionic liquids [18]. The electrochemical stabilities and ionic conductivities of imidazolium-based mono-ether functional ionic liquids were also dependent on the sizes and structures of constituent anions and cations [37].

Bester-Rogač et al. carried out studies on a series of alkylimidazolium ionic liquids in DMSO, methanol [38], water, dichloromethane (DCM) and acetonitrile [39, 40] to investigate their transport and aggregation properties. Boruń et al. carried out the electrical conductance studies of imidazolium based tetrafluoroborate ILs ([emim][BF₄] and [bmim][BF₄]) as a function of temperature (283.15-318.5 K) in various solvents like water, DCM, N,N-dimethylformamide, 1-propanol etc. [16, 36, 41, 42]. Ionic conductivities of these IL-molecular solvent binary mixtures were found to increase with the temperature. Kalugin et al. carried out conductometric studies of a series of imidazolium ILs in acetonitrile [43]. The conductivity values increased with the rise in temperature and decreased as the size of the constituent ions increased [43]. The same group later carried out a comparative study on the conductivity of imidazolium, ammonium and pyridinium based ionic liquids in methanol [44]. The long alkyl chain containing ammonium ILs displayed lower conductivities in methanol compared to the imidazolium and pyridinium based ILs. Seki et al. investigated the effects of cations and anions on the physical properties of 12 room-temperature ionic liquids. It was found that variation of the physical properties of RTILs was greatly affected by the cation species due to their molecular structural changes (single bond, double bond, chainlike, or cyclic) and conformation (planar or non-planar), compared to that for the anion species [45].

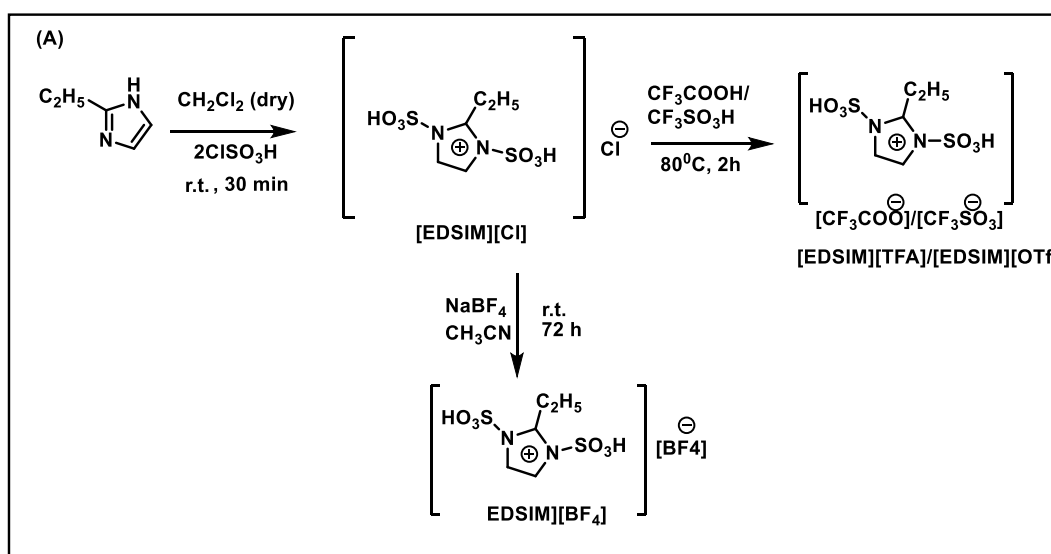
In our present work, we explored the effects of varied combinations of cations (2-ethyl-1,3-disulfoimidazolium, N, N-disulfodiethylammonium and N, N-disulfodibutylammonium) and anions (Cl⁻, CF₃COO⁻, OTf⁻, BF₄⁻) on the physicochemical properties of ILs like density, Brønsted acidity, ionic conductivity, electrochemical stability window, polarity, moisture sensitivity and thermal stability of the ionic liquids. The ionic conductivities and electrochemical stability windows (ESWs) of the 12 Brønsted acidic ionic liquids (BAILs) were measured in three molecular solvents acetone, MeCN and MeOH. The variation of conductivity values of binary mixtures of IL were correlated to the Kamlet-Taft solvatochromic parameters of these

molecular solvents. Cyclic Voltammetry (CV) technique was employed to measure the ESWs of the IL solutions and the results were correlated with the change in molecular structures of the constituent ions and the interactions of constituent ion-pairs of the ILs with the molecular solvents.

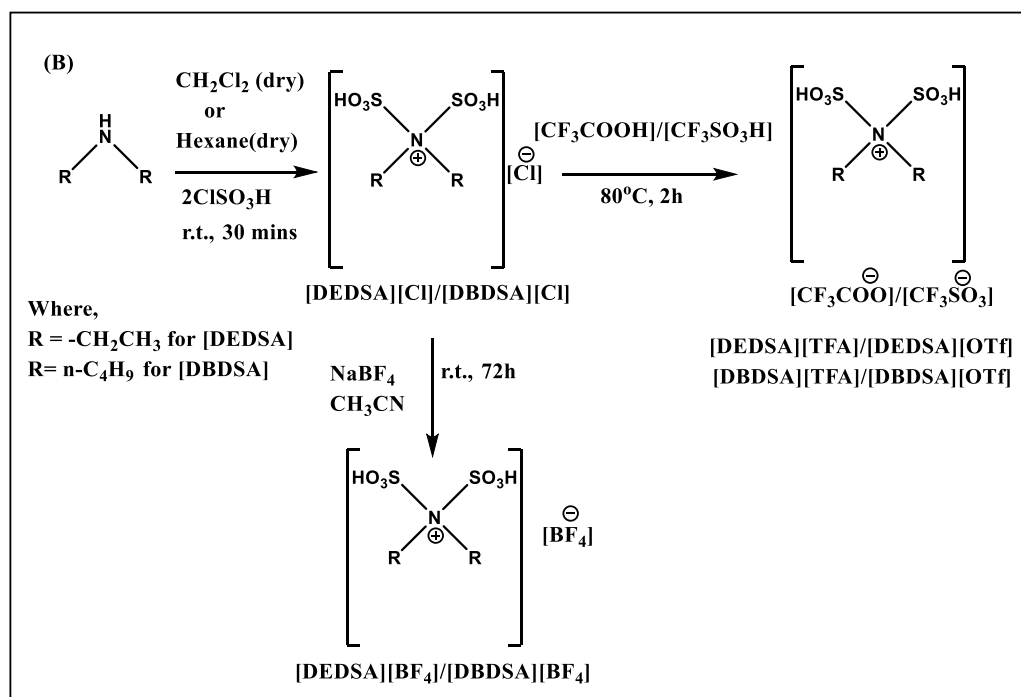
4.2 Results and Discussion

4.2.1 Characterization of the N-SO₃H functionalized Brønsted acidic ionic liquids (BAILs)

In this work, 3 reported and 9 new N-SO₃H functionalized BAILs of ammonium and imidazolium cations with the four anions (Cl⁻, BF₄⁻, CF₃COO⁻ and OTf⁻) were synthesized according to the optimized methods given in experimental section (**Scheme 4.1 A & B**). The BAILs characterized by using analytical techniques like FT-IR and NMR (¹H, ¹³C, ¹⁹F).



Scheme 4.1(A): Synthesis of $-\text{SO}_3\text{H}$ functionalized 2-ethyl-1,3-disulfoimidazolium ([EDSIM]) based ILs.



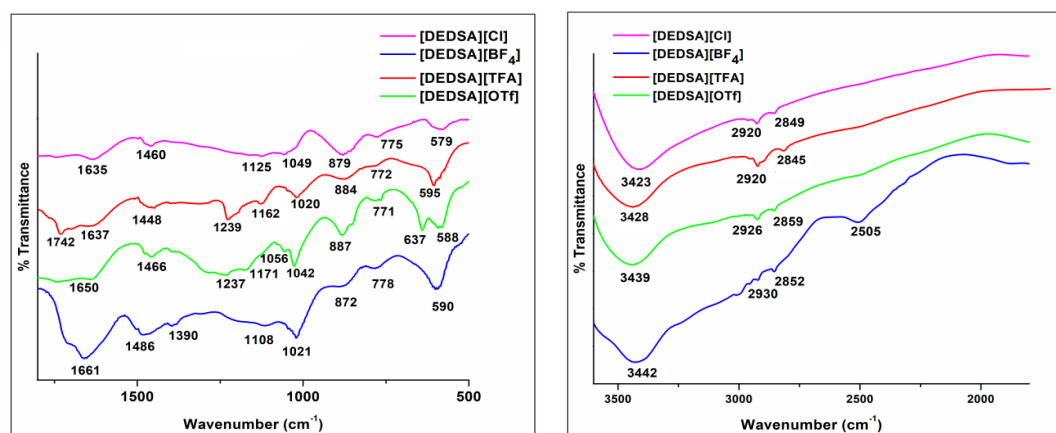
Scheme 4.1 (B): Synthesis of $-\text{SO}_3\text{H}$ functionalized ammonium ([DEDSA]/[DBDSA]) based ILs.

4.2.1.1 FT-IR analysis

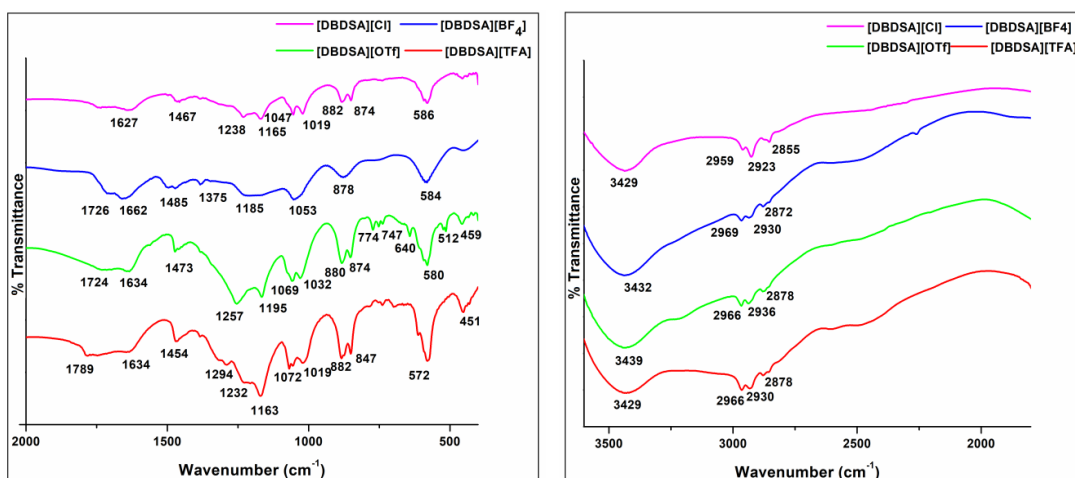
FT-IR spectra of the 12 ionic liquids were recorded in the region of $500\text{--}4000\text{ cm}^{-1}$. **Fig.4.1 (A, B & C)** displays the FT-IR spectra of [DEDSA], [DBDSA] and [EDSIM] ILs respectively. The FT-IR band assignments of the BAILs are listed in **Table 4.1**.

Table 4.1: FT-IR band assignments of the BAILs.

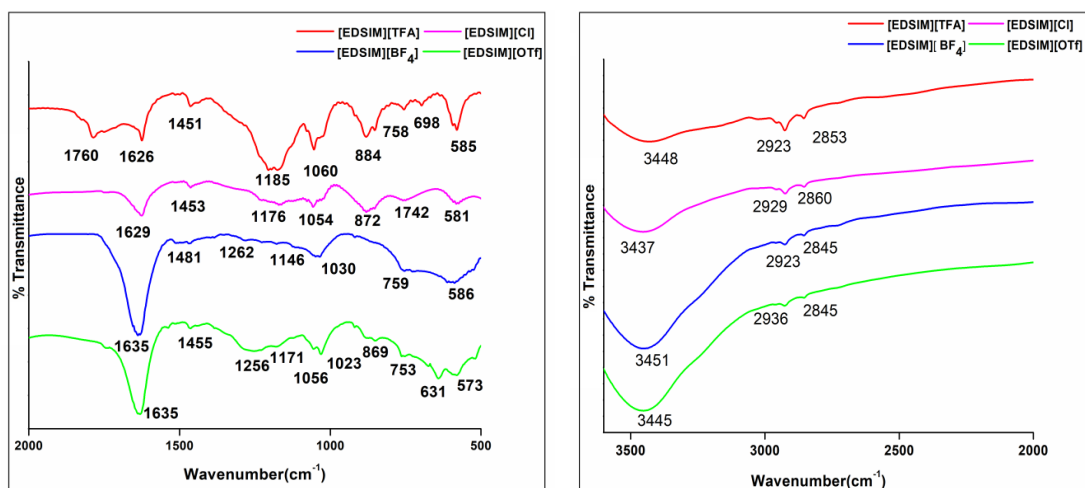
Peaks (cm^{-1})	Assignments
572–587	$-\text{SO}_3\text{H}$ (bending)
750–760	out of plane ring bending of $-\text{CH}$ bond
870–885	N-S stretching
1040–1060	S-O symmetric stretching
1178–1192	S-O asymmetric stretching
1200–1340	C- N stretching
1441–1468	C-H bending of $-\text{CH}_3$ group
1640–1620 (strong)	$-\text{C}=\text{C}-$ stretching
1650–1600 (weak)	H-O-H bending of physisorbed water observed in case of ammonium based ILs
1730–1790	C=O stretching
2910–2929	C-H stretching
3450–3400	$-\text{OH}$ stretching due to intermolecular H-bonding among IL molecules



A



B



C

Fig. 4.1: FT-IR spectra of (A) [DEDSA] ionic liquids (B) [DBDSA] ionic liquids and (C) [EDSIM] ionic liquids.

4.2.1.2 NMR analysis

The proton (^1H) NMR spectra of the 8 ammonium ILs ([DEDSA] and [DBDSA]) displayed a single 2 proton signal near 8.1-8.5 ppm confirming attachment of the two $-\text{SO}_3\text{H}$ groups to the organic cations through N atom. For the imidazolium ILs ([EDSIM]) a similar ^1H NMR signal for $-\text{SO}_3\text{H}$ groups bound to the nitrogen of the imidazolium cation was observed around 12.9-13.9 ppm. Other characteristic ^1H NMR peaks of the imidazolium and ammonium cations were also observed in aromatic and aliphatic regions respectively. The ^{13}C NMR spectra of the ILs also displayed the characteristic peaks in both the aliphatic and aromatic regions based on the nature of the carbon present. The ^{13}C NMR of all the trifluoroacetate anion containing ILs displayed a peak near 159 ppm corresponding to the carbonyl carbon of the trifluoroacetate anion. The ^{19}F spectra of $[\text{BF}_4]^-$ anion containing ILs showed characteristic peak near -148 ppm confirming the presence of $[\text{BF}_4]^-$ anion. **Section 4.4.3** shows the NMR spectra (^1H , ^{13}C & ^{19}F) of the ILs [DBDSA][TFA] and [EDSIM] $[\text{BF}_4]$.

4.2.2 Investigation of the physicochemical properties of the BAILs

4.2.2.1 Thermogravimetric analysis (TGA)

Thermogravimetric plots of the [DEDSA], [DBDSA] and [EDSIM] ionic liquids are represented in **Fig.4.2 (A, B & C)** The [DEDSA][TFA] and [DEDSA][Cl] showed identical TGA plots with a mass loss of around 19 % and 12 % respectively, corresponding to the physisorbed water near 100 °C. It was followed by another degradation at 250 °C. Similar type of TGA plots were also observed for the trifluoroacetate and chloride based ILs of [DBDSA] and [EDSIM] cations. These plots revealed highly hydrophilic nature of the trifluoroacetate ILs. The strong H-bonding ability of trifluoroacetate anion increases the hydrophilic nature of trifluoroacetate ILs. All the six ILs of CF_3COO^- and Cl^- anions were found to be thermally stable up to 250 °C.

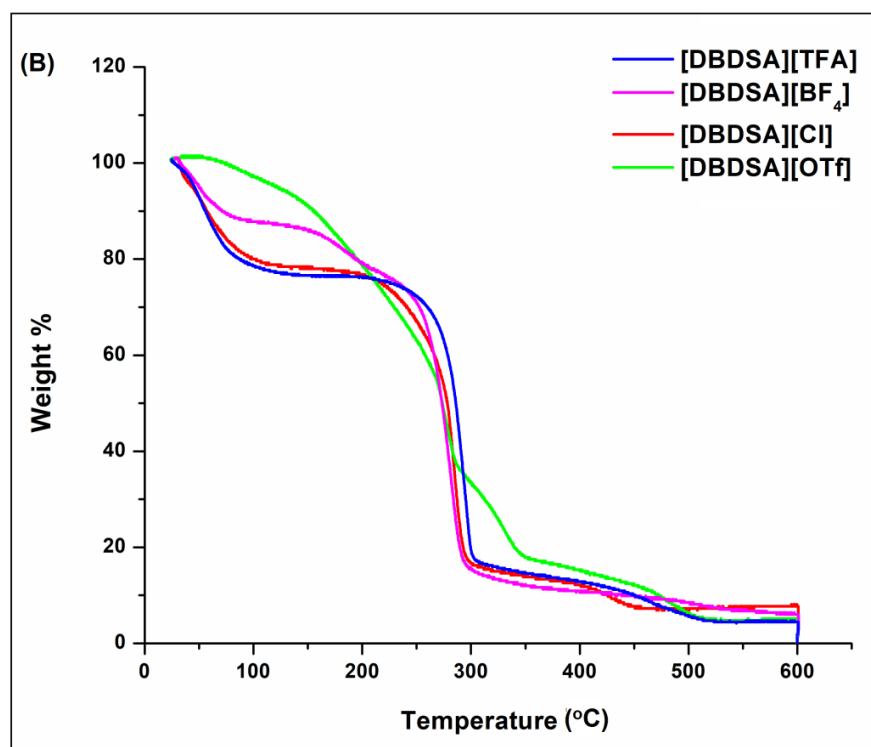
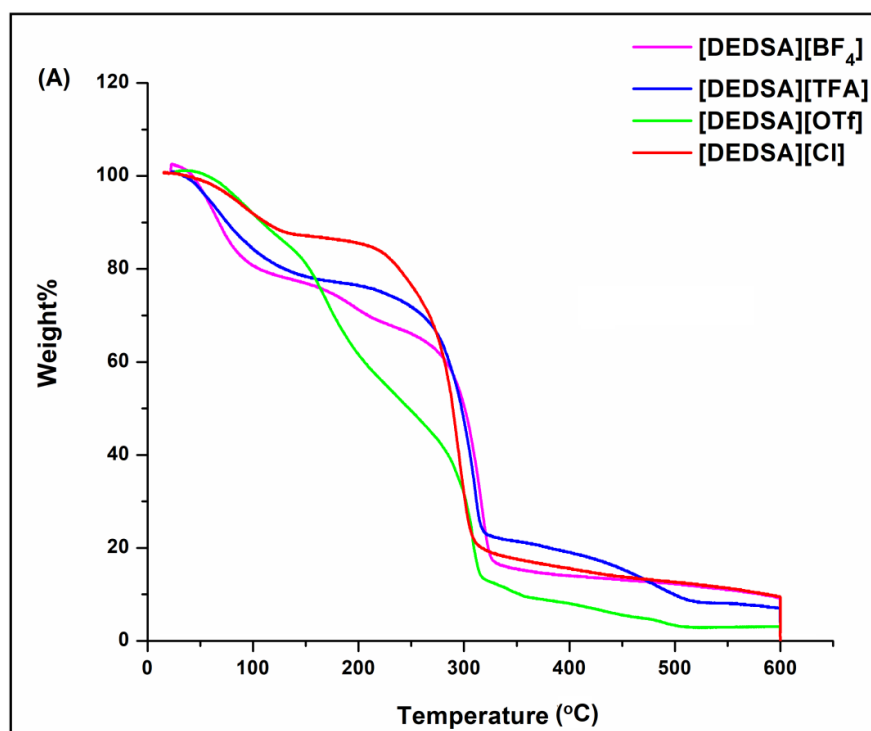
The weak coordinating ability of the $[\text{BF}_4]^-$ anion [46] with the N,N-disulfodialkylammonium cations, resulted in the gradual loss of mass about 19.5 % around 72°C and 12.4 % around 77 °C in the TGA plots of [DEDSA][BF_4] and [DBDSA][BF_4] respectively, followed by subsequent decomposition above 150 °C. The TGA curve pattern of the [DEDSA][BF_4] revealed it to be less thermally stable

compared to [DBDSA] [BF₄]. This can be attributed to the increasing stability of the [DBDSA] cation, which is based on two factors: (i) increasing +I inductive effect of the butyl group and (ii) increasing number of hyperconjugation structures of the [DBDSA] cation. At the same time, the imidazolium based [EDSIM][BF₄] ionic liquid seemed to release only 7% moisture near 100 °C and showed thermal stability up to 170 °C. The higher thermal stability of [EDSIM][BF₄] can be attributed to the stable aromatic character of 2-ethylimidazolium cation with its delocalised resonating structures which can provide sufficient ionic strength between the ion pair despite weak coordinating ability of the [BF₄]⁻ anion.

TGA profiles of the three [OTf]⁻ anion containing ILs with dialkylammonium ([DEDSA] & [DBDSA]) and ethyl imidazolium ([EDSIM]) cations expressed a slow decomposition starting around 100 °C to till 300 °C and 350 °C respectively. This can be attributed to the weak coordinating ability of [OTf]⁻ anion similar to [BF₄]⁻, which reduces their interionic strength in the respective ionic liquids [46]. The inertness of [BF₄]⁻ anion arises from its symmetrical structure with equal distribution of negative charge over the four electronegative fluorine atoms. Similarly, the weak coordinating nature of the [OTf]⁻ anion results from the delocalization of negative charge over the three oxygen atoms and the presence of electron withdrawing -CF₃ group. Furthermore, these anions are excellent leaving groups and can easily be replaced by other ligands (like H₂O) under very mild conditions [46, 47]. The TGA curves show that even slight amount of moisture causes the decomposition of [BF₄]⁻ and [OTf]⁻ anions based ionic liquids having weaker interionic strength between the ion-pair at slightly elevated temperatures.

Water content of the BAILs

The water content in the 12 BAILs were determined from their TGA (**Fig. 4.2**) and TGA-derivative curves (**Fig. 4.3**). The derivative curves allow us to correctly evaluate the first event of a mass loss in the graph, which occurs due to evaporation of moisture. All the derivative curves show a peak in the 60-100 °C regions indicating the loss of water. The weight loss between 60-100 °C is taken as the weight of water and the residual weight is taken as the weight of the ionic liquid. The calculated results are presented in **Table 4.2**.



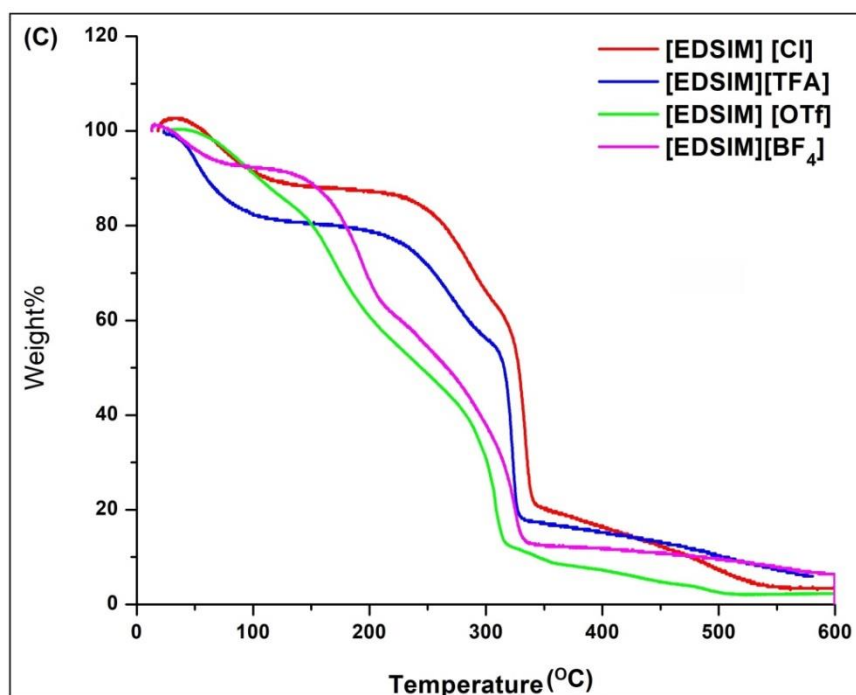
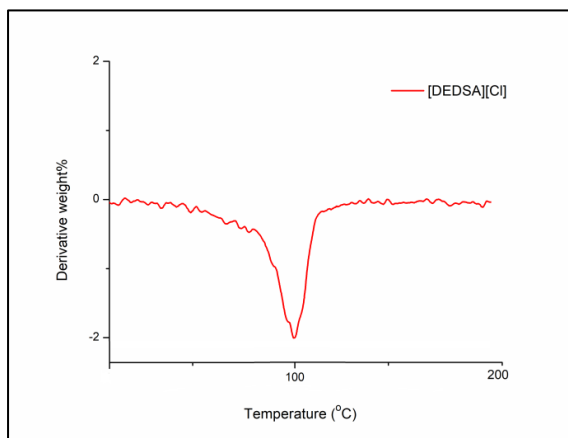


Fig. 4.2: TGA plots of (A) Diethylammonium [DEDSA] based ILs (B) Dibutylammonium [DBDSA] based ILs (C) Ethylimidazolium [EDSIM] based ILs.

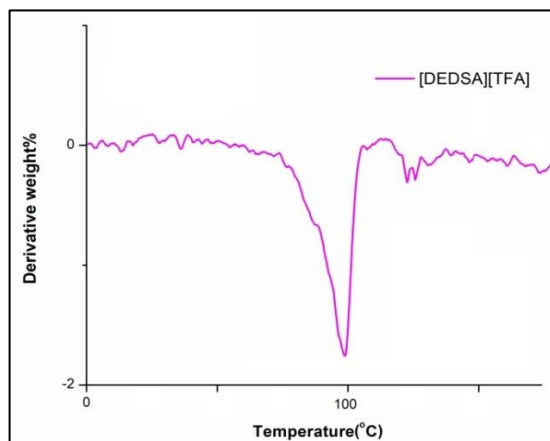
Table 4.2: Water content of the BAILs obtained from TGA and derivative curves.

Entry	Ionic Liquid	Water Content (wt%) ^{a,b}	Empirical formula
1	[DEDSA][Cl]	12.1	[DEDSA][Cl].2 H ₂ O
2	[DEDSA][TFA]	19	[DEDSA][TFA].5 H ₂ O
3	[DEDSA][OTf]	8	[DEDSA][OTf]. 2 H ₂ O
4	[DEDSA][BF ₄]	19.5	[DEDSA][BF ₄].4 H ₂ O
5	[DBDSA][Cl]	19.4	[DBDSA][Cl].4 H ₂ O
6	[DBDSA][TFA]	20	[DBDSA][TFA]. 6 H ₂ O
7	[DBDSA][OTf]	4	[DBDSA][OTf]. H ₂ O
8	[DBDSA][BF ₄]	12.4	[DBDSA][BF ₄].3H ₂ O
9	[EDSIM][Cl]	9.7	[EDSIM][Cl].2H ₂ O
10	[EDSIM][TFA]	15	[EDSIM][TFA].4 H ₂ O
11	[EDSIM][OTf]	6.1	[EDSIM][OTf]. H ₂ O
12	[EDSIM][BF ₄]	7.6	[EDSIM][BF ₄].H ₂ O

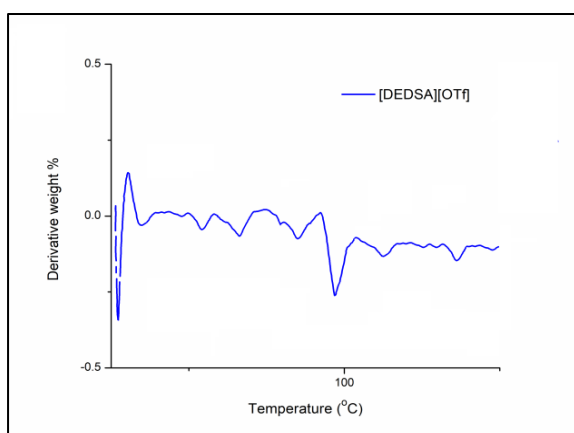
^a Drying of ILs were conducted for 10h (entries 1,3,7,9,11& 12). ^b Drying of ILs was done for 24 h (entries 2, 4,5, 6, 8 & 10).



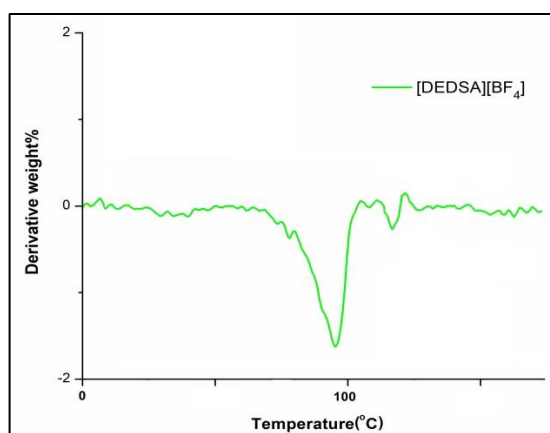
(A)



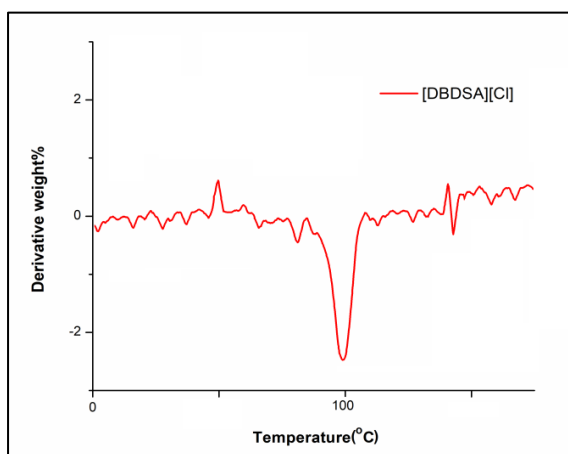
(B)



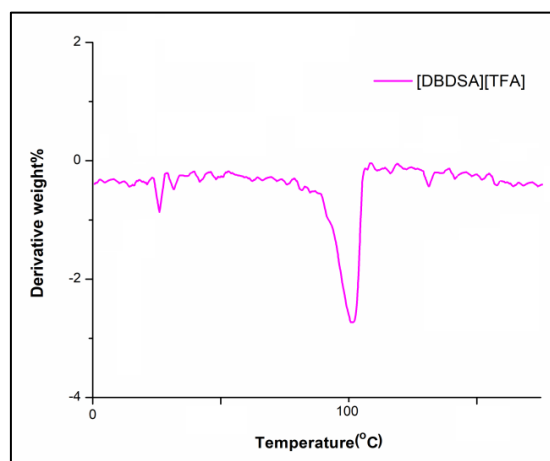
(C)



(D)



(E)



(F)

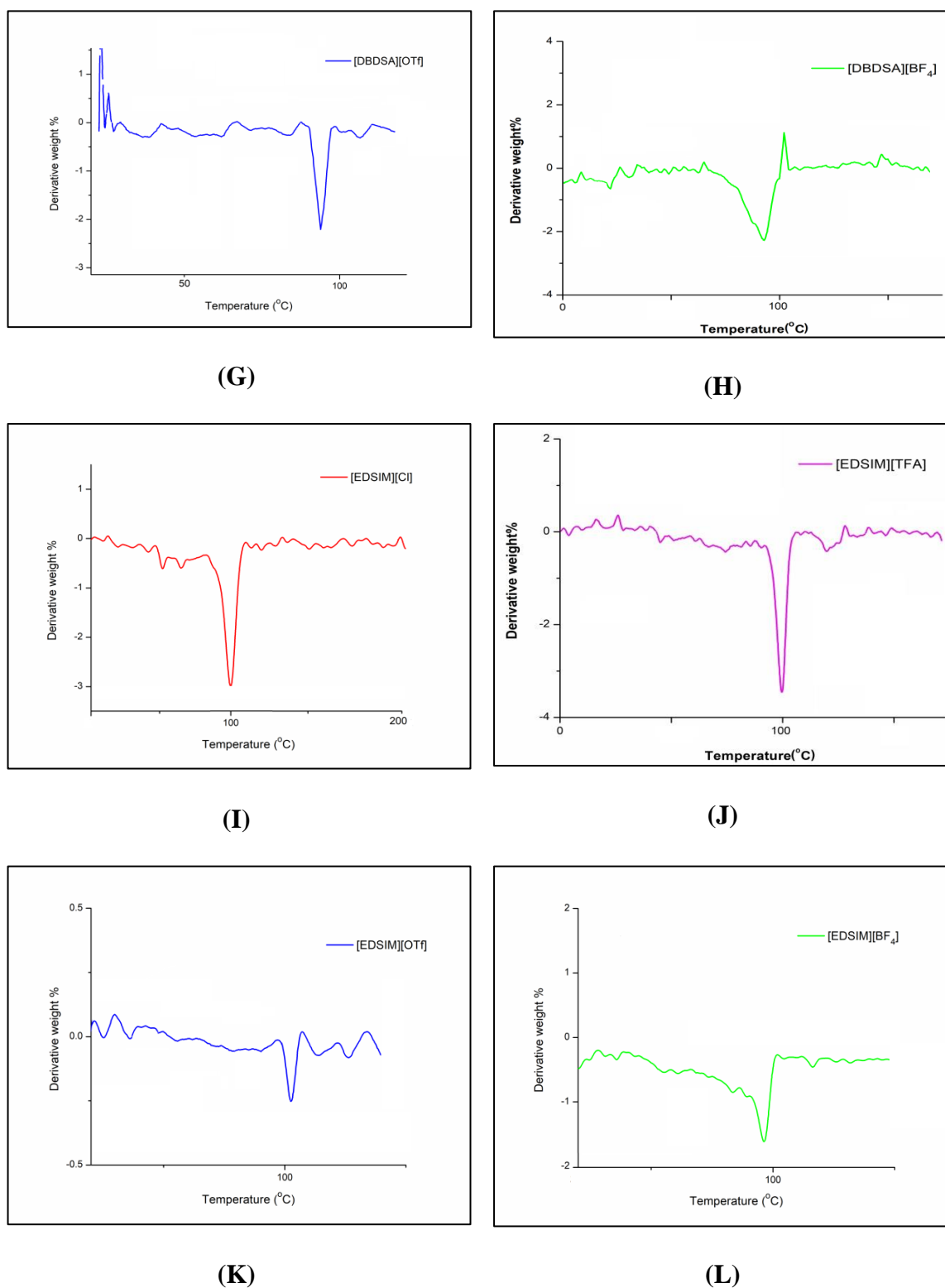


Fig. 4.3: Derivative TGA curves of (A) [DEDSA][Cl] (B) [DEDSA][TFA] (C) [DEDSA][OTf] (D) [DEDSA][BF₄] (E) [DBDSA][Cl] (F) [DBDSA][TFA] (G) [DBDSA][OTf] (H) [DBDSA][BF₄] (I) [EDSIM][Cl] (J) [EDSIM][TFA] (K) [EDSIM][OTf] (L) [EDSIM][BF₄].

4.2.2.2 Hammett acidity of the BAILs

The Brønsted acidities of the three series of BAILs were determined from their UV-visible Hammett plots (**Fig.4.4 A, B & C**) by calculating Hammett acidity functions (H^0) using the **Equation 1.4** from **Chapter 1**. The lowering of observed H^0 values for any IL indicates the increase of acidic strength among all the ILs. **Table 4.3** contains the calculated H^0 values of all the ILs and it displayed slightly higher H^0 values for the [DBDSA] series as compared to the comparable H^0 values of other two series i.e. [DEDSA] and [EDSIM] based ILs. These observations revealed somewhat less acidic nature of the [DBDSA] series among the three series of ILs. This may be expected as an outcome of the reduction of electron deficient character of the ammonium cation with increasing +I effect of bulkier sized N-butyl substituents for the N,N-disubstituted ammonium ILs.

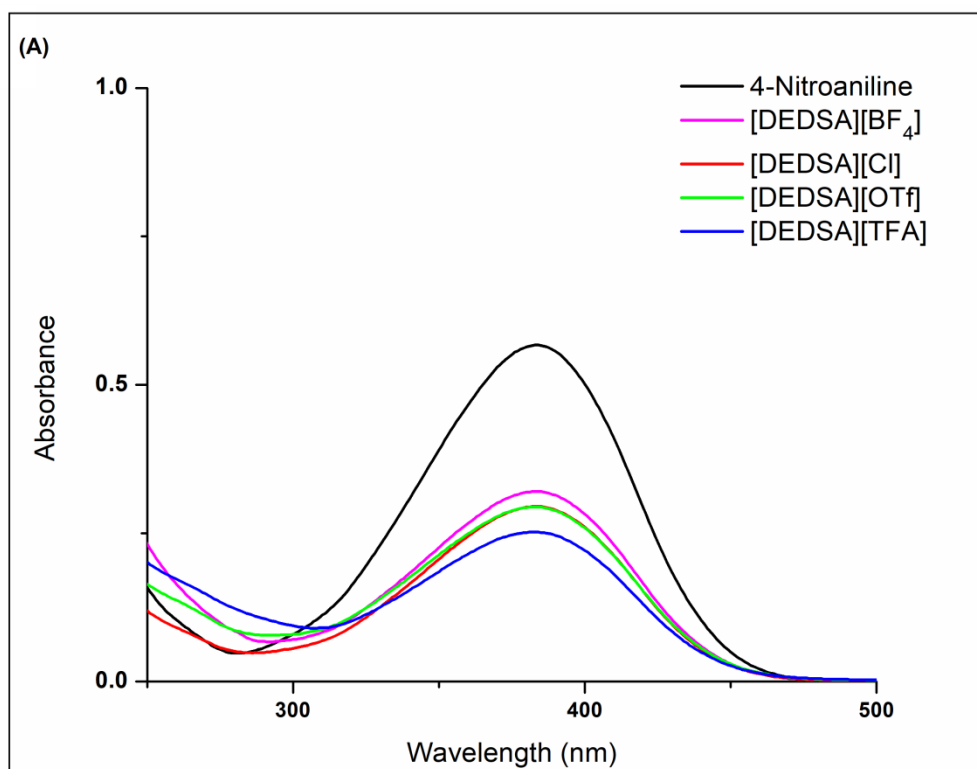
Among the four counter anions, the $[CF_3COO]^-$ anion is responsible for moderately higher acidic nature of the ionic liquids as it delivers an electron deficient nature to the organic cations compared to the of $[Cl]^-$ and $[OTf]^-$ anions. The delocalized structures of carboxylate anion may provide more ionic interactions with the organic cations increasing the electron deficient characters and thus raising their acidities.

The ILs containing $[BF_4]^-$ anion were the least acidic ones in each of the three series. This might be due to the weakly-coordinating nature of the $[BF_4]^-$ anion, which decreases the electron deficient character of the cations and hence, their acidity. In the previous **Chapter 3** we compared the Brønsted acidity of the [EDSIM][TFA] and [EDSIM][Cl] with that of the unsubstituted [DSIM][TFA] and [DSIM][Cl]. As expected, the [EDSIM] ILs were less acidic than the [DSIM] ILs owing to the reduction of electron deficient character of the imidazolium cation with the increasing +I inductive effect of the C-2 substituent.

Table 4.3: Hammett acidity functions (H^0) of the BAILs.

Entry	IL	A_{max}	[I]%	[HI]%	H^0
1	4-Nitroaniline	0.57	100	-	-
2	[DEDSA][Cl]	0.29	52.20	47.80	1.03
3	[DEDSA][BF ₄]	0.32	56.43	43.57	1.10

4	[DEDSA][TFA]	0.25	44.44	55.56	0.89
5	[DEDSA][OTf]	0.28	51.85	48.15	1.02
6	[DBDSA][Cl]	0.31	54.49	45.51	1.07
7	[DBDSA][BF ₄]	0.34	60.14	39.86	1.17
8	[DBDSA][TFA]	0.27	49.38	50.62	0.98
9	[DBDSA][OTf]	0.32	55.55	44.45	1.09
10	[EDSIM][Cl]	0.28	50.79	49.21	1.00
11	[EDSIM][BF ₄]	0.35	59.96	40.04	1.16
12	[EDSIM][TFA]	0.25	44.79	55.21	0.90
13	[EDSIM][OTf]	0.29	52.38	47.62	1.03



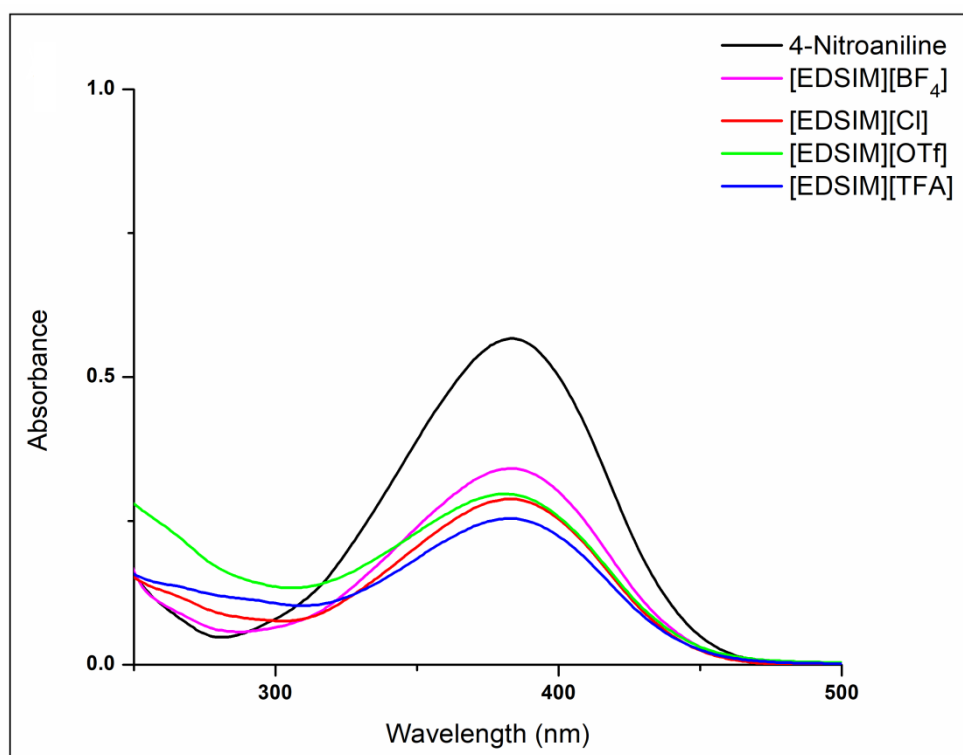
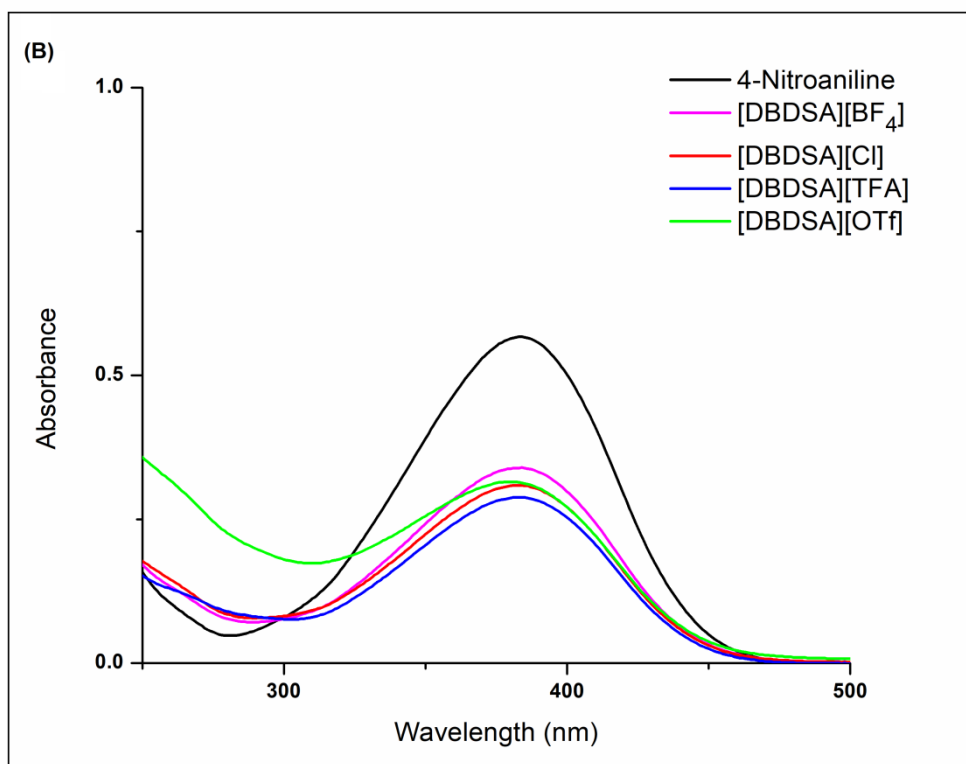


Fig. 4.4: Hammett acidity plots of (A) DEDSA series (B) DBDSA series and (C) EDSIM series.

4.2.2.3 Electrochemical stability of the BAILs in molecular solvents

The Cyclic Voltammograms (CVs) of 0.1 M solution of the 12 BAILs in MeOH, MeCN and acetone were recorded at room temperature using glassy carbon as the working electrode and Ag/Ag⁺ as the reference electrode. The CV plots for the [DEDSA], [DBDSA] and [EDSIM] series in the three molecular solvents are shown in **Fig. 4.5**, **4.6** and **4.7**. The electrochemical stability windows (ESWs) of the binary mixtures of ILs in molecular solvents are calculated from their corresponding CV plots (**Fig. 4.5**, **4.6** and **4.7**) using **Equation 1.3** from the **chapter 1**. The values of the ESWs obtained are included in **Table 4.4 (A, B & C)**. The electrochemical stability of the ion-pairs of 12 ionic liquids in molecular solvents was affected by the variation of solvent-solute interactions as well by the nature of constituent ions, which is discussed below under different sub-sections.

Effect of solvent

Among the three molecular solvents acetone, MeOH and MeCN, the ILs exhibited comparable electrochemical stability in both the MeCN and acetone. However, the cathodic limits of the ILs increase significantly in case of acetone as seen from the **Fig. 4.5**, **4.6 & 4.7**. There must be some favourable H-bonding interactions occurring between the carbonyl oxygen of the acetone and the sulfonic groups of organic cations, which probably increases the cathodic stability of ILs [48].

Additionally, methanol also provides a stabilizing effect to the organic cations through H-bonding interactions with the -SO₃H groups resulting in increased cathodic limits. However, the strength of such interactions is less in MeCN and hence, a decrease in their cathodic limits is observed as can be seen from the **Table 4.4 (A, B, C)**. Furthermore, MeOH also causes the electrochemical oxidative degradation of the anions to radical intermediates by providing a hydrogen radical H[•] to produce HCl, CF₃COOH, CF₃SO₃H and HBF₄ as smaller molecules. This is the most probable reason for their reduced anodic limits. The absence of acidic proton in MeCN and acetone increases the limits of the anodic potentials. The electrochemical stability windows (ESWs) of the ILs in acetone are in the range of 2.66-2.88 V for the DEDSA and DBDSA series and 3.03-3.45 V for the EDSIM series.

Table 4.4A: ESW of the [DEDSA] ILs calculated from the observed cathodic and anodic potentials.

Solvent	Ionic Liquids	E_{anodic} (V)	E_{cathodic} (V)	E.S.W. (V)
MeCN	[DEDSA][Cl]	1.57	-1.03	2.59
	[DEDSA][TFA]	1.63	-1.06	2.69
	[DEDSA][BF ₄]	1.43	-1.09	2.52
	[DEDSA][OTf]	1.68	-1.05	2.73
Acetone	[DEDSA][Cl]	1.29	-1.54	2.83
	[DEDSA][TFA]	1.23	-1.65	2.88
	[DEDSA][BF ₄]	1.28	-1.50	2.78
	[DEDSA][OTf]	1.26	-1.40	2.66
MeOH	[DEDSA][Cl]	1.08	-1.33	2.41
	[DEDSA][TFA]	1.03	-1.34	2.37
	[DEDSA][BF ₄]	1.20	-1.41	2.61
	[DEDSA][OTf]	1.05	-1.35	2.40

Effect of cation

For the two series of ammonium ILs, the ESWs slightly increased with increasing sizes of the N-alkyl chain length. This effect was observed more or less in all the three molecular solvents. The cathodic stabilities of the [DBDSA] ionic liquids were found to be slightly higher in all the three studied molecular solvents compared to the [DEDSA] ionic liquids. This increase in the reductive stability of ILs can be attributed to the +I inductive effect of the alkyl substituents [49-52].

Among the three series of ILs, the [EDSIM] series had the highest ESW ranges in acetone (3.07-3.45 V) and CH₃CN (2.75-3.42 V). However, their electrochemical stability in MeOH is significantly lower compared to the ammonium ILs, with their reductive stability stooping to as low as -0.11V in case of [EDSIM][BF₄]. Their anodic stability in MeOH is however, similar to that of other eight ILs. Thus, the EDSIM series is found to be more electrochemically stable than the ammonium ILs in aprotic solvents

like acetone and CH₃CN, but their electrochemical stability decreases in the protic MeOH.

However, on comparing our results with those in the Chapter 3, we observe the electrochemical stability of the [EDSIM] series ionic liquids are greater than the reported unsubstituted 1,3-disulfoimidazolium ILs. This again can be attributed to the increasing reductive stability of 1,3-disulfo-2-ethyl imidazolium cation by the +I inductive effect of ethyl group [49-51].

Table 4.4B: ESW of the [DBDSA] ILs calculated from the observed cathodic and anodic potentials.

Solvent	Ionic Liquids	E _{anodic} (V)	E _{cathodic} (V)	E.S.W. (V)
Acetone	[DBDSA][Cl]	1.04	-1.63	2.67
	[DBDSA][TFA]	1.31	-1.61	2.92
	[DBDSA][BF ₄]	1.23	-1.59	2.83
	[DBDSA][OTf]	1.25	-1.64	2.89
MeOH	[DBDSA][Cl]	1.21	-1.29	2.50
	[DBDSA][TFA]	1.28	-1.35	2.63
	[DBDSA][BF ₄]	1.06	-1.39	2.45
	[DBDSA][OTf]	1.09	-1.32	2.41
MeCN	[DBDSA][Cl]	1.70	-1.16	2.86
	[DBDSA][TFA]	1.51	-1.15	2.66
	[DBDSA][BF ₄]	1.47	-1.25	2.72
	[DBDSA][OTf]	1.44	-1.18	2.62

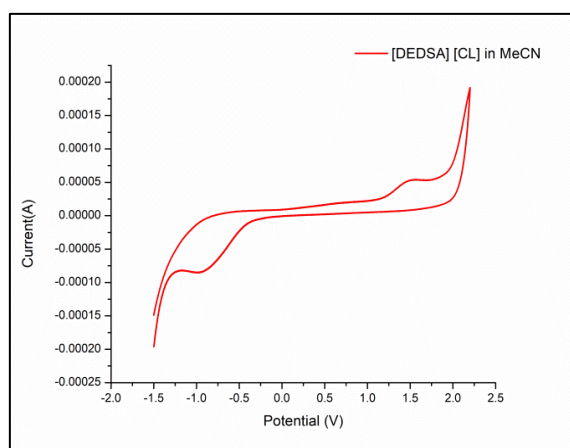
Effect of anion

All the four anions [CF₃COO]⁻, [OTf]⁻, [BF₄]⁻ and [Cl]⁻ in these ILs have shown comparable anodic stability and are seen to vary with the cation and solvent used as seen from Fig. 4.5, 4.6 & 4.7. and Table 4.4 (A, B & C). Similar anodic stability is to be

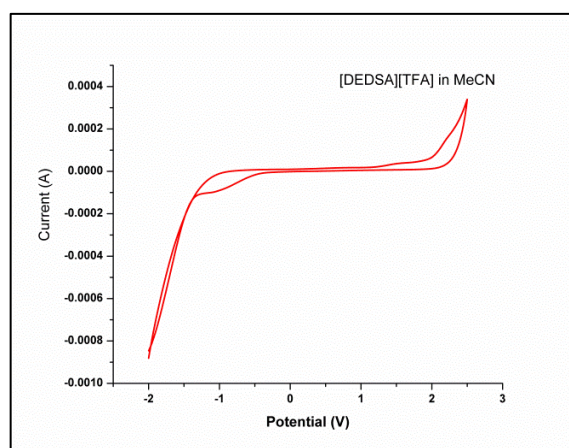
expected for the ILs having the same anion [52]. However, this is not the case, and we observe that for a given solvent, the ILs with the same anion shows different anodic potentials and this is somehow influenced by their respective cations [52, 53].

Table 4.4C: ESW of the [EDSIM] ILs calculated from the observed cathodic and anodic potentials.

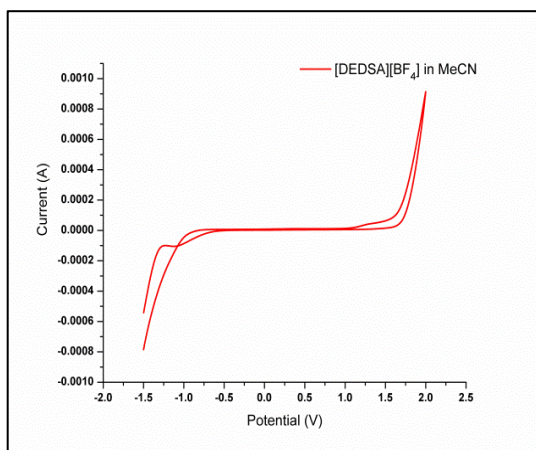
Solvent	Ionic liquid	$E_{\text{anodic}}(\text{V})$	$E_{\text{cathodic}}(\text{V})$	E.S.W.(V)
MeCN	[EDSIM][Cl]	1.51	-1.24	2.75
	[EDSIM][TFA]	1.54	1.30	2.84
	[EDSIM][OTf]	1.80	-1.37	3.17
	[EDSIM][BF ₄]	2.12	-1.30	3.42
MeOH	[EDSIM][Cl]	1.18	-0.22	1.40
	[EDSIM][TFA]	1.16	-0.22	1.38
	[EDSIM][OTf]	1.12	-0.25	1.37
	[EDSIM][BF ₄]	1.08	-0.11	1.19
Acetone	[EDSIM][Cl]	1.85	-1.60	3.45
	[EDSIM][TFA]	1.69	-1.61	3.30
	[EDSIM][OTf]	1.61	-1.70	3.31
	[EDSIM][BF ₄]	1.55	-1.52	3.07



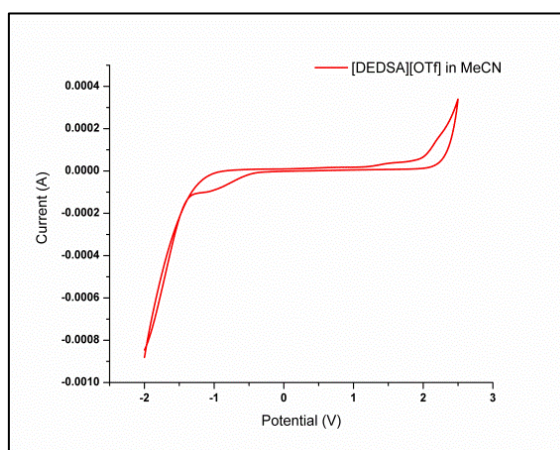
(A)



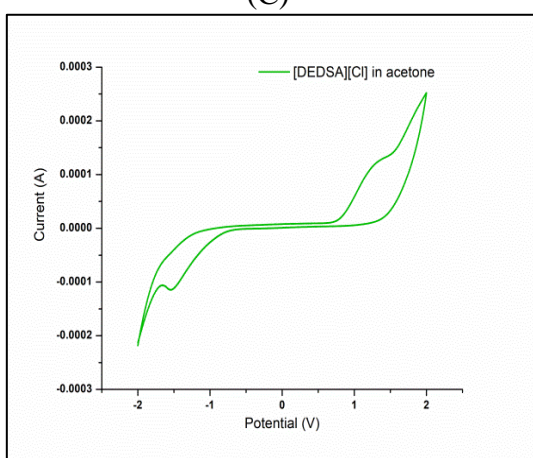
(B)



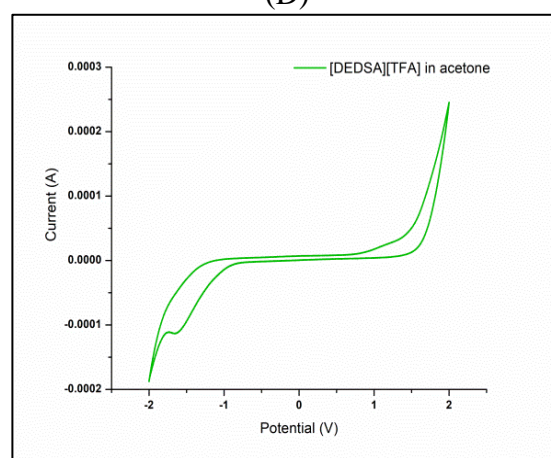
(C)



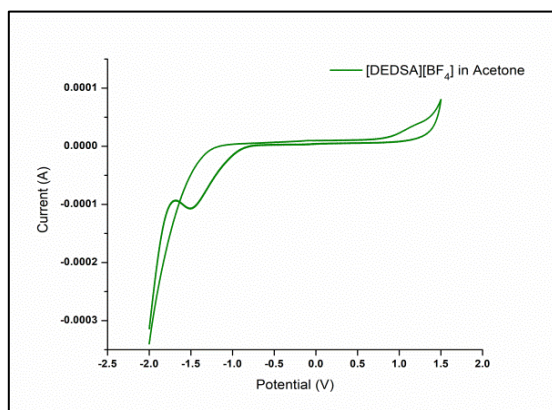
(D)



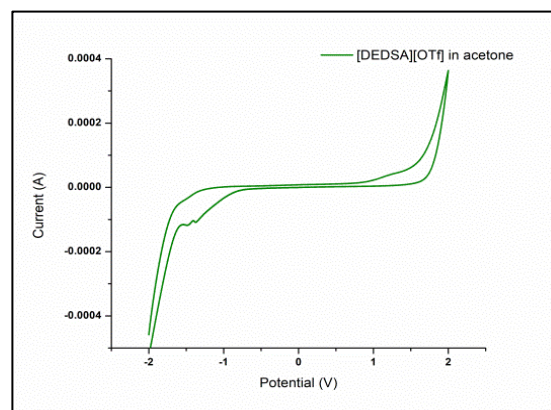
(E)



(F)



(G)



(H)

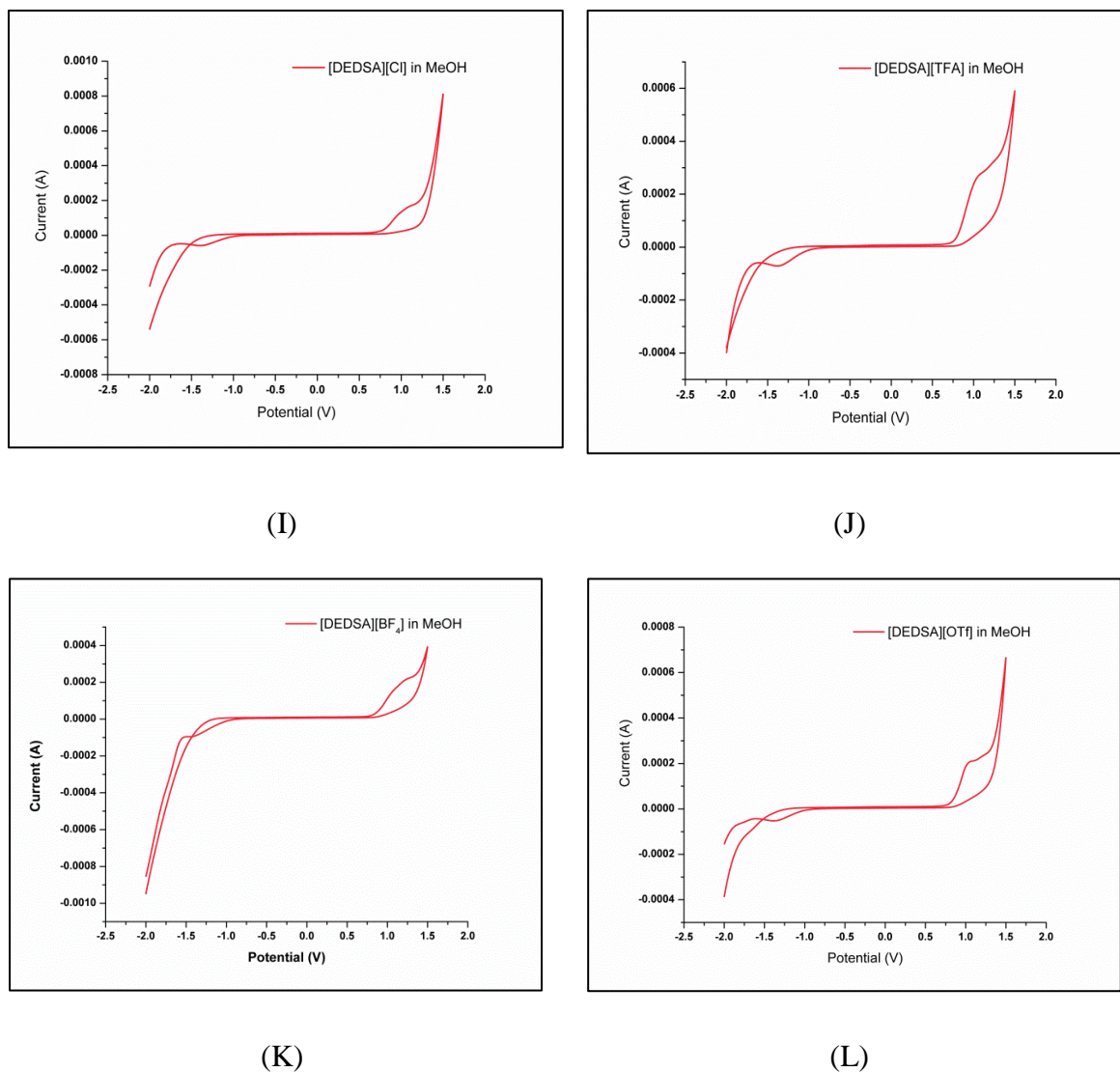
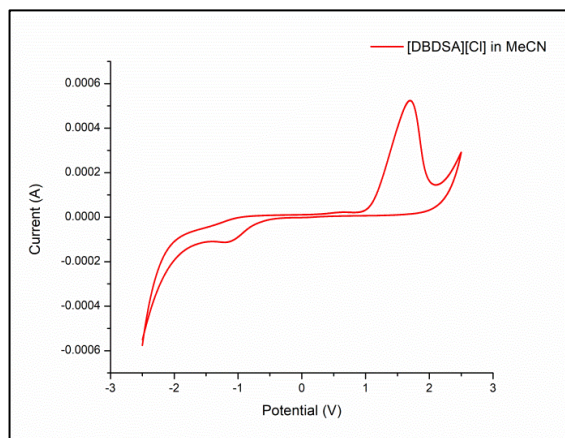
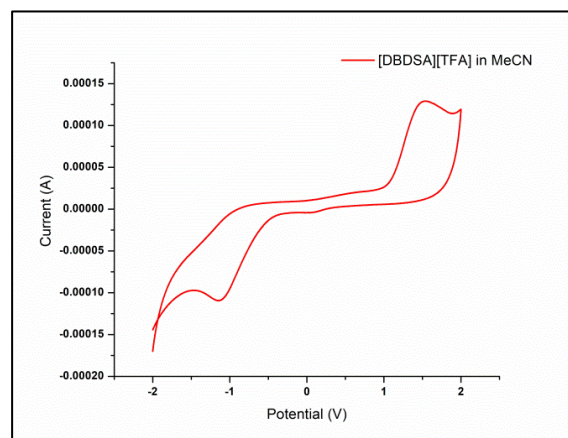


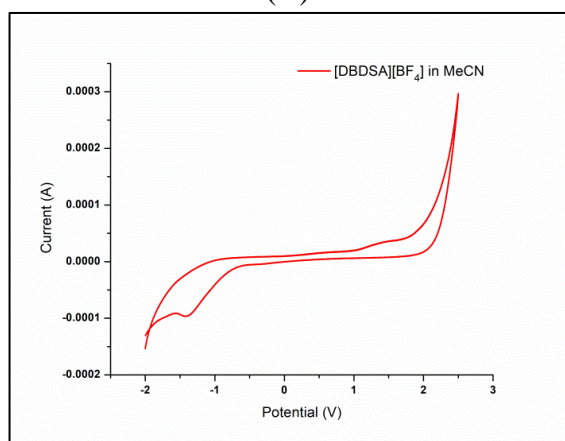
Fig. 4.5: Plot of electrochemical window of ionic liquids (A) [DEDSA][Cl] in MeCN (B) [DEDSA][TFA] in MeCN (C) [DEDSA][BF₄] in MeCN (D) [DEDSA][OTf] in MeCN (E) [DEDSA][Cl] in acetone (F) [DEDSA][TFA] in acetone (G) [DEDSA][BF₄] in acetone (H) [DEDSA][OTf] in acetone (I) [DEDSA][Cl] in MeOH (J) [DEDSA][TFA] in MeOH (K) [DEDSA][BF₄] in MeOH (L) [DEDSA][OTf] in MeOH.



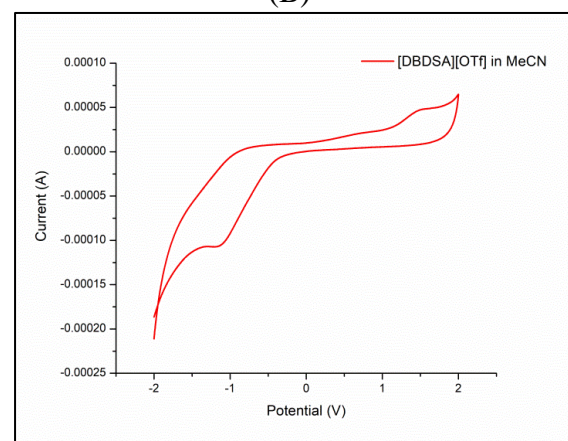
(A)



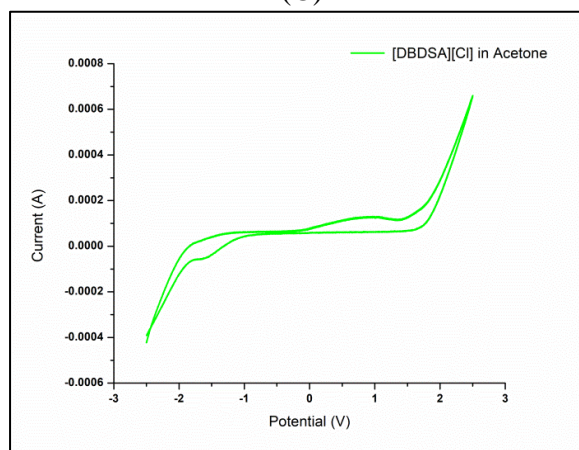
(B)



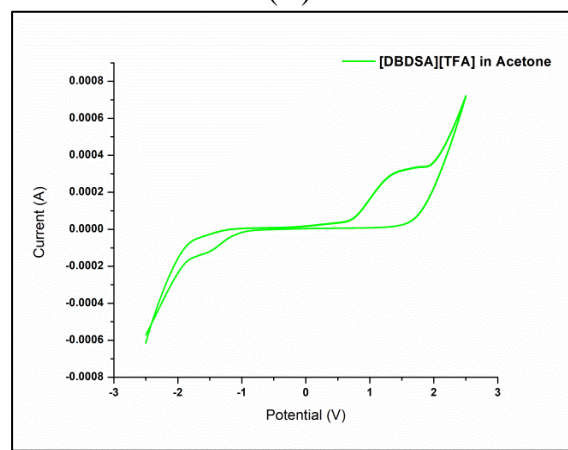
(C)



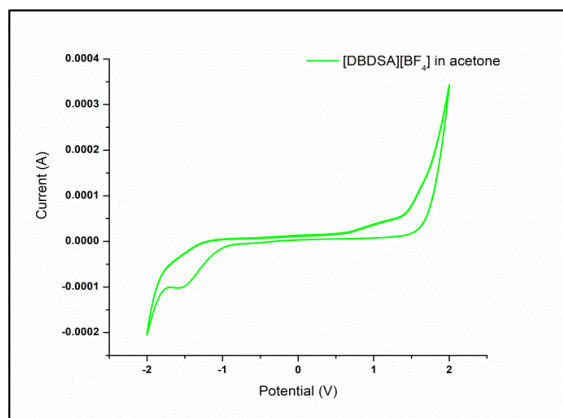
(D)



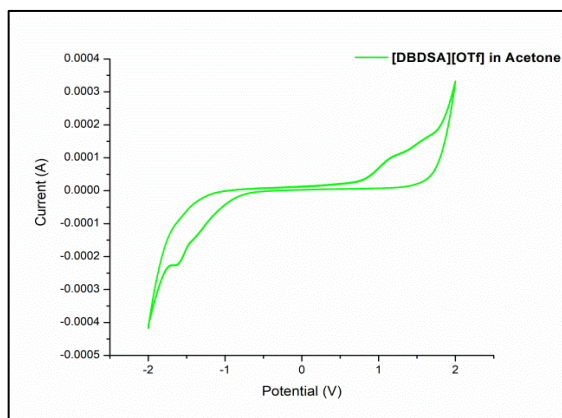
(E)



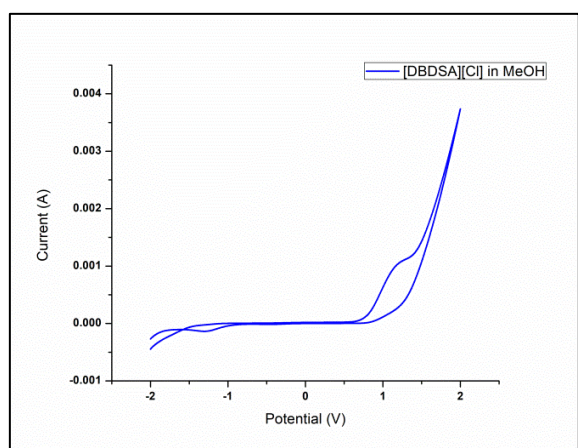
(F)



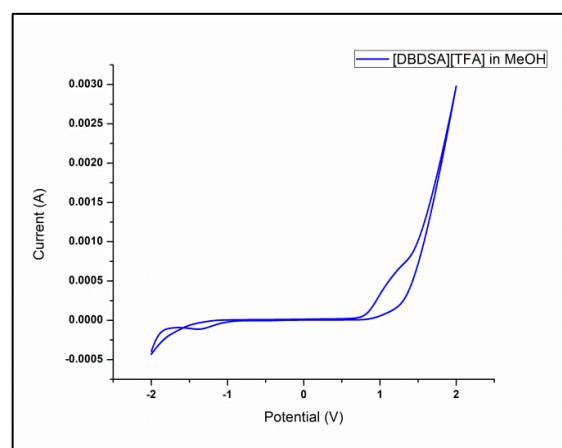
(G)



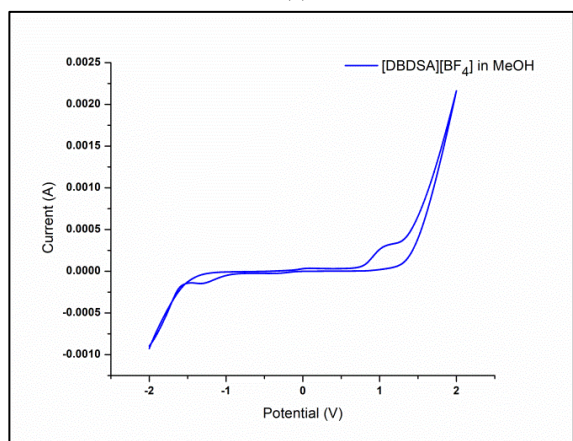
(H)



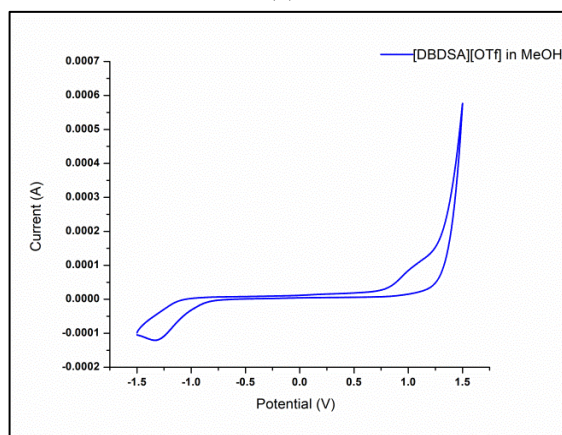
(I)



(J)

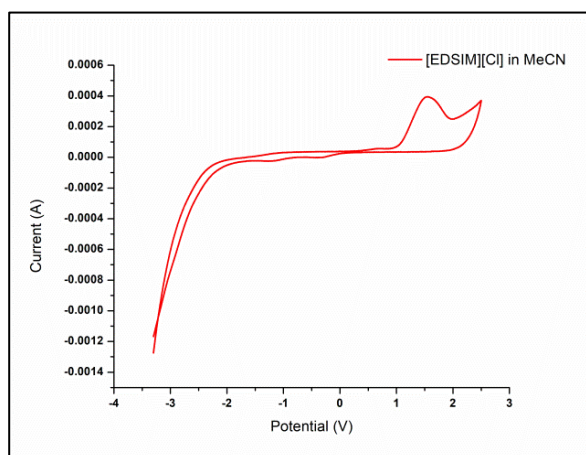


(K)

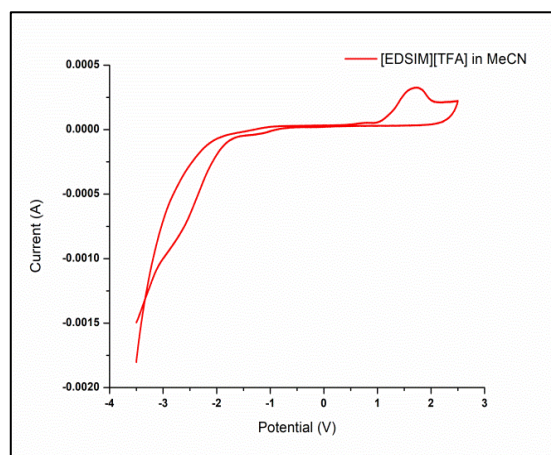


(L)

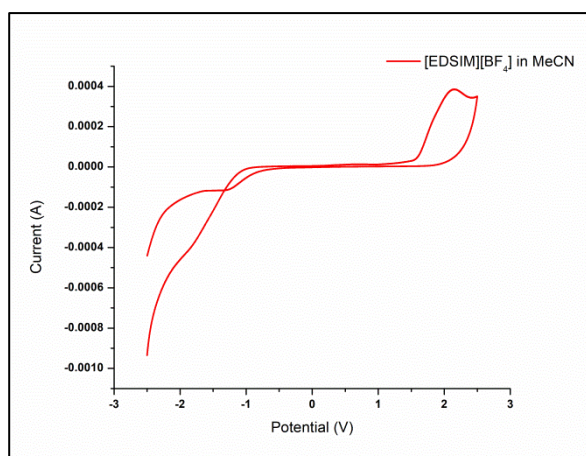
Fig. 4.6: Plot of electrochemical window of ionic liquids (A) [DBDSA][Cl] in MeCN (B) [DBDSA][TFA] in MeCN (C) [DBDSA][BF₄] in MeCN (D) [DBDSA][OTf] in MeCN (E) [DBDSA][Cl] in acetone (F) [DBDSA][TFA] in acetone (G) [DBDSA][BF₄] in acetone (H) [DBDSA][OTf] in acetone (I) [DBDSA][Cl] in MeOH (J) [DBDSA][TFA] in MeOH (K) [DBDSA][BF₄] in MeOH (L)[DBDSA][OTf] in MeOH.



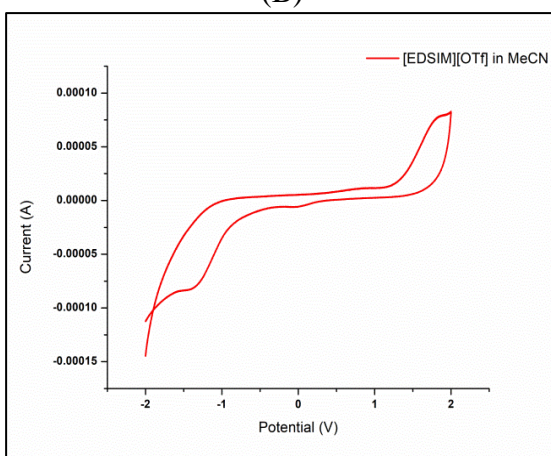
(A)



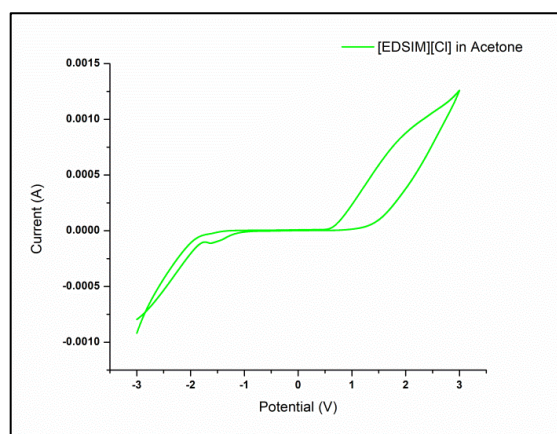
(B)



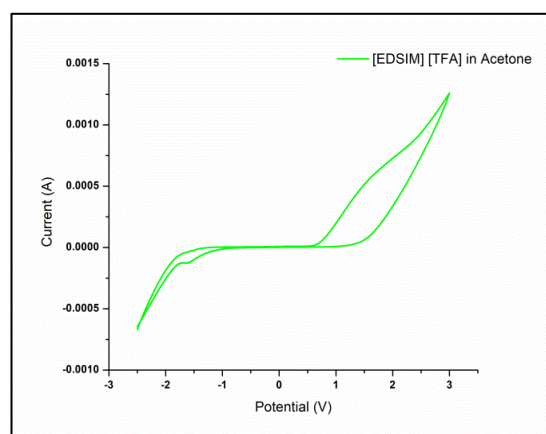
(C)



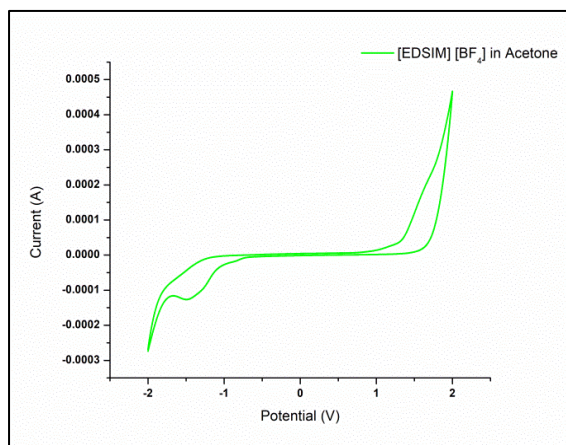
(D)



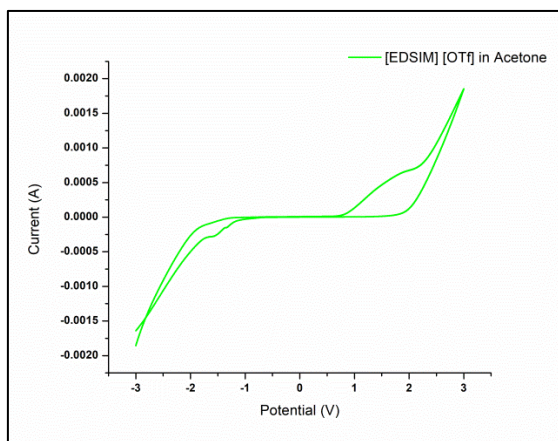
(E)



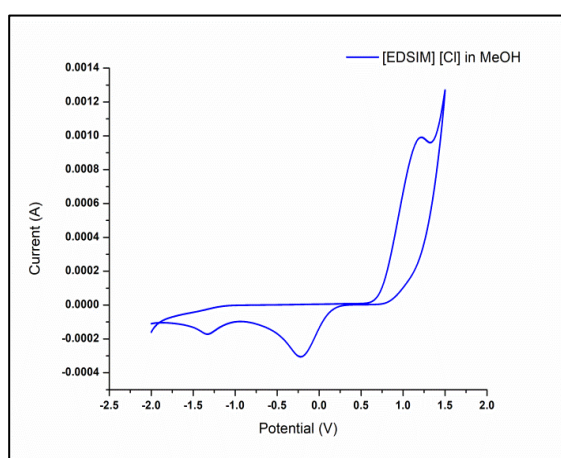
(F)



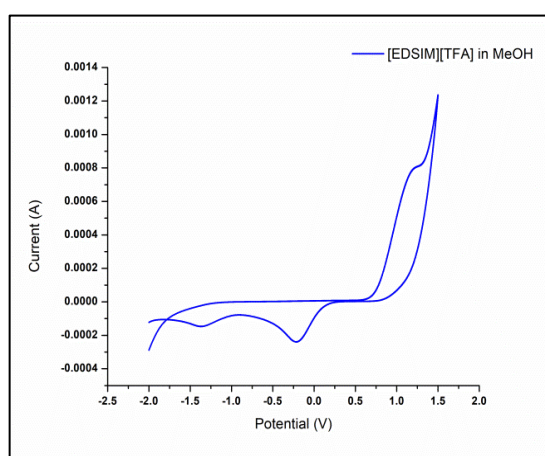
(G)



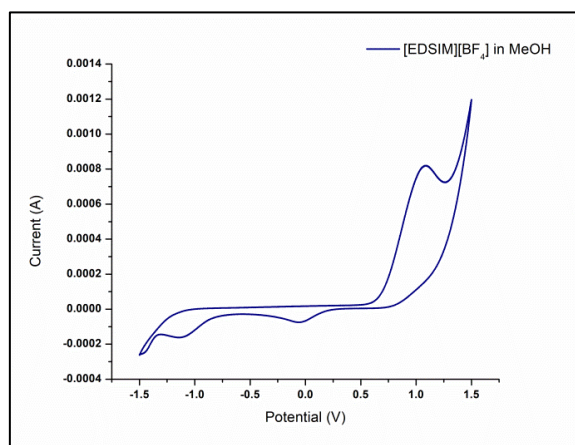
(H)



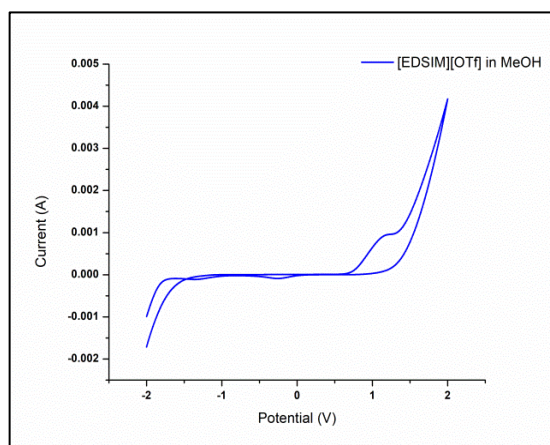
(I)



(J)



(K)



(L)

Fig. 4.7: Plot of electrochemical window of ionic liquids (A) [EDSIM][Cl] in MeCN (B) [EDSIM][TFA] in MeCN (C) [EDSIM][BF₄] in MeCN (D) [EDSIM][OTf] in MeCN (E) [EDSIM][Cl] in acetone (F) [EDSIM][TFA] in acetone (G) [EDSIM][BF₄] in acetone

(H) [EDSIM][OTf] in acetone (I) [EDSIM][Cl] in MeOH (J) [EDSIM][TFA] in MeOH (K) [EDSIM][BF₄] in MeOH (L) [EDSIM][OTf] in MeOH .

4.2.2.4 Conductivity of the BAILs in molecular solvents

The conductivities (σ) of the twelve BAILs were measured in three molecular solvents acetone, acetonitrile, and methanol at 298.15 K (**Table 4.5**). It was found that the conductivities of ILs were affected by their constituent ions and the nature of molecular solvent used [16, 36].

Table 4.5: Conductivity of the 12 ionic liquids in MeOH, MeCN and acetone (mole fraction $x_{IL} = 0.001$) at 298.15 K.

Ionic liquid	Conductivity in MeOH (mScm ⁻¹)	Conductivity in MeCN (mScm ⁻¹)	Conductivity in acetone (mScm ⁻¹)
[EDSIM][Cl]	2.83	0.96	0.37
[EDSIM][TFA]	3.90	1.00	0.42
[EDSIM][OTf]	2.85	0.97	0.39
[EDSIM][BF ₄]	4.27	2.42	0.94
[DEDSA][Cl]	2.06	0.78	0.23
[DEDSA][TFA]	2.26	0.86	0.24
[DEDSA][OTf]	2.19	0.84	0.25
[DEDSA][BF ₄]	2.62	0.95	0.30
[DBDSA][Cl]	1.57	0.46	0.10
[DBDSA][TFA]	1.71	0.57	0.12
[DBDSA][OTf]	1.54	0.49	0.12
[DBDSA][BF ₄]	1.91	0.65	0.20

Effect of solvent

The conductivity of the ionic liquids in molecular solvents varies with the polarity of the respective solvent. The overall polarity of a solvent can be expressed in terms of the Kamlet-Taft solvatochromic relationship which describes the contribution of hydrogen bond donor (α), hydrogen bond acceptor (β) properties of solvents and Dimroth-Richardt's $E^T(30)$ values to the overall solvent polarity of solution, as explained in the sub-section 3.2.2.4 of Chapter 3.

The known solvatochromic parameter values (**Table 4.6**) of MeOH, MeCN and acetone were utilized for analysing the variation in conductivity (**Table 4.5**) of the twelve ILs in these molecular solvents at a particular mole fraction of the ILs, $x_{IL} = 0.001$ at 298.15 K [16, 54, 55]. It was noticed that the conductivity (σ) of the ionic liquid solutions increases with rising polarity order of the solvent represented by their values of E_N^T as: Acetone < MeCN < MeOH.

Additionally, the intermolecular H-bond formation ability of the protic co-solvent MeOH with the $-SO_3H$ groups of these ILs, stabilizes the constituent ions of each of the IL. This enhances the electrical conductivities of the binary mixtures of IL-MeOH compared to those of IL-acetone and IL-MeCN. The presence of intermolecular H-bonding interactions between the protic solvent (MeOH) with the constituent ions of the ILs is largely responsible for separation of the ion pair with increasing numbers of “free” ions and thus, favouring an increase in the conductivities of the IL-MeOH mixtures. Hence, it can be concluded that the solvation of cations and anions of the ILs in these solvents are mainly controlled by the hydrogen-bond donor ability (α) of the solvent which plays a crucial role in their conductivity [16]. A similar role is also played by the H-bond acceptor ability (β) of the solvent. Thus, it can be concluded that the high H-bond donor (α) and acceptor (β) ability of MeOH increase the conductivity values of the binary mixtures of the IL solution in MeOH.

Table 4.6: Solvatochromic parameters of molecular solvents at 298.15 K.

Solvent	E_N^T	α	β
MeOH	0.762	1.05	0.61
MeCN	0.460	0.38	0.39
Acetone	0.355	0.10	0.50

Effect of cation

Among the three series of ILs, the imidazolium ILs showed the highest conductivity in the three molecular solvents (**Table 4.5**). The [EDSIM] series was followed by the N,N-disulfodiethylammonium ILs. The N,N-disulfodibutylammonium ILs had the lowest conductivity values among the three, in all the molecular solvents used. This can be attributed to the fact that mobility of the ions gradually decreases with their increasing

size and hence conductivity lowers [19, 36]. Both types of N,N-disulfodialkylammonium ILs have bulkier cations compared to the 2-alkyl, 1,3-disulfoimidazolium ILs.

Effect of anion

Although the effect of cation sizes was predominant over the type of anions used, but still the effect of anion type on the conductivity values was also observed for the three IL series. The maximum ionic conductivities were observed for the binary mixtures of $[\text{BF}_4]^-$ anion based ILs in these solvents. This can be attributed to the greater mobility of the $[\text{BF}_4]^-$ ion due to its small size. However, the size of anions is not the only factor governing their conductivities, as the ILs of $[\text{Cl}]^-$ anion have lower conductivities than those having $[\text{CF}_3\text{COO}]^-$ ion. This might be related to the self-aggregation of ions that do not contribute to the ionic conductivity [56]. The increasing degree of dissociation of the ILs increase their overall ionic conductivity. Ion dissociation increases as anion polarity decreases, owing to the reduced role of electrostatic forces acting on a given ion pair. An anion's ability to donate electron density (Lewis basicity) is a measure of its polarity [56, 57]. From the available literature, it has been found that $[\text{Cl}]^-$ has greater basicity and hence greater polarity compared to the $[\text{CF}_3\text{COO}]^-$, $[\text{OTf}]^-$ and $[\text{BF}_4]^-$ ions. This is in accordance with our conductivity results [56-58].

4.2.2.5 Polarity study of the BAILs with Fluorescence probe

Polar nature of the synthesized ionic liquids was evaluated by taking fluorescence emission spectrum of pyrene as a probe molecule in two exemplifying ionic liquids $[\text{EDSIM}][\text{Cl}]$ and $[\text{EDSIM}][\text{TFA}]$ in **Fig. 4.8 (A & B)**. Pyrene is a highly fluorescent aromatic compound and is often used as a probe in solvent-polarity studies. The fluorescence emission spectrum of pyrene is characterized by five major vibronic bands designated as **Bands I, II, III, IV** and **V**, with well-defined peaks at ~375, 379, 385, 395 and 410 nm, respectively [59]. These are monomeric emission peaks and some of them are very solvent sensitive. **Band III** is immensely sensitive to the polarity of the probe's microenvironment and displays an increase in the fluorescence emission intensity in comparison to that of **Band I** in hydrophobic environments. The **Band I** however gains considerable intensity in polar solvents. The ratio of **Band III** to **Band I** is a good qualitative measure of solvent polarity and its value decreases with increase in solvent polarity [60]. In the **Fig.4.8 (A & B)**, we observe that only a broad, unstructured excimer band appeared at longer wavelengths (ranging from 425-450 nm) for pyrene in the IL

medium. The excimers or ‘excited-state dimers’ appear around 440-550 nm and are formed as a result of the interactions between a ground state and an excited state pyrene ring which are ~ 10 Å apart from each other [59]. Unusually long lifetime of pyrene emission (50–90 ns) facilitates the formation of such excimers. These excimers can offer key insights to the physicochemical properties of solubilizing environment. The pyrene fluorescence emission spectra of both [EDSIM][Cl] and [EDSIM][TFA] in **Fig 4.8 (A & B)** don’t show any characteristic monomer emission peaks. Thus, no ratio of **Band III** to **Band I** could be determined for these ionic liquids. However, it can be concluded that the ionic liquids must be of highly polar nature, as polar solvents are known to stabilize the excimer state and reduce the energy barrier of excimer formation [61-63].

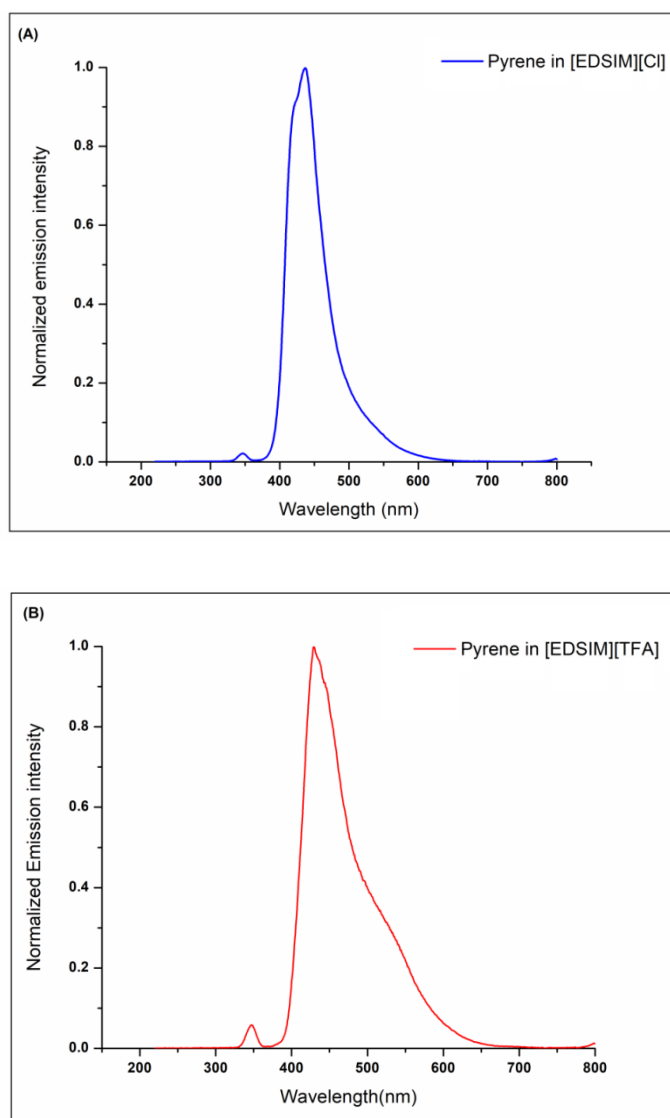


Fig. 4.8: Fluorescence emission spectra of pyrene (excitation wavelength = 345 nm) in (A) [EDSIM] [Cl] (B) [EDSIM][TFA].

4.2.2.6 Density of the ILs

Densities of the BAILs were measured using a pycnometer at 25 °C. The density values are presented in **Table 4.7**.

Table 4.7: Density of Ionic liquids

Sl No.	Ionic liquid	Density [g/cm ³]
1	[EDSIM][Cl]	1.49
2	[EDSIM][TFA]	1.59
3	[DBDSA][Cl]	1.35
4	[DBDSA][TFA]	1.38
5	[DEDSA][Cl]	1.40
6	[DEDSA][TFA]	1.49

The densities of the 2-ethylimidazolium cation based ILs [EDSIM][Cl] and [EDSIM][TFA] were found to be higher than the ammonium based ILs. This can be attributed to the fact that a compact packing is possible in case of the imidazolium rings which is not possible in case of the linear chain ammonium ionic liquids [64, 65]. As a result, the free space between two ammonium-based IL molecules increases and hence, the density decreases. The compactness decreases with the increase in chain length of the alkyl groups and therefore, the dibutyl ammonium based ionic liquids are found to be less dense compared to the diethylammonium based ionic liquids. In case of the anions, the trifluoroacetate based ionic liquids were found to be slightly denser than their chloride counterparts in each case. Densities of the [OTf]⁻ and [BF₄]⁻ based ILs couldn't be measured because of their paste like consistency.

4.3 Summary

In this work, we compared the various physicochemical properties of N-SO₃H functionalized imidazolium and ammonium ILs. Twelve members of N-SO₃H functionalized ammonium and imidazolium based Brønsted acidic ionic liquids were synthesized and subjected for analysis of their physical and electrochemical properties after their characterization by ¹H NMR, ¹³C NMR, and FT-IR techniques. The compact packing of the imidazolium rings is absent in case of the linear chain ammonium ionic

liquids which led to an increase in the density of the 2-ethylimidazolium ILs. The six of the Cl⁻ and TFA anion based ionic liquids showed similar thermal stability up to 250-260°C, whereas the other six BF₄⁻ and OTf⁻ anion based ILs were found to be less thermally stable due to the weakly coordinating nature of the anions. The water content of the ILs was determined using their TGA and first derivative curves. The TFA based ILs expressed maximum hydrophilic character. The evaluation of the Hammett acidity functions (H⁰) of the ILs revealed comparable and almost similar H⁰ functions for [DEDSA] and [EDSIM] series of the ILs. The [DBDSA] series was however slightly less acidic compared to the other two due to the increasing +I effect of the N-alkyl substituent of the ammonium cation. Cyclic Voltammetry study displayed wider ESWs of the BAILs in acetone and MeCN as compared to MeOH at the same temperature. Among the two ammonium IL series, the ESWs of the [DBDSA] ILs in all the three molecular solvents were found to be slightly higher than the [DEDSA] ILs. This can be attributed to the increase in the electrochemical stability of the [DBDSA] ILs with the size of the alkyl chain length. The [EDSIM] series had the highest ESW in acetone (3.07-3.45 V) and MeCN (2.75-3.42 V) among the three series of ILs. The pyrene fluorescence emission spectra of [EDSIM][Cl] and [EDSIM][TFA] showed a broad structureless band corresponding to excimer emission with its peak around 440-450 nm confirming their highly polar nature, responsible for stabilising the excimer state of pyrene. The conductivity of the twelve ionic liquids at a particular concentration (mole fraction $x_{IL}=0.001$) and temperature (298.15 K) in the molecular solvents varies with the polarity of the respective solvent, size of the ions and presence of ion-pair aggregates. Among the three series of ILs, the imidazolium based ILs ([EDSIM] series) showed the highest conductivity in the three molecular solvents, which was followed by the [DEDSA] series and then the [DBDSA] series. This study shows a potential for these functionalized ILs to be used as suitable candidates for electrolyte materials in various electrochemical devices in their pure state and also as binary mixture with molecular solvents. Moreover, their acidic nature along with other interesting properties like high thermal and chemical stability make them eligible to be used as catalysts various organic reactions.

4.4 Experimental Section

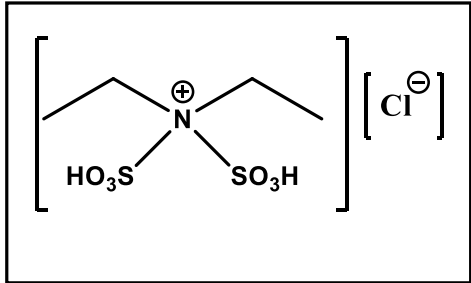
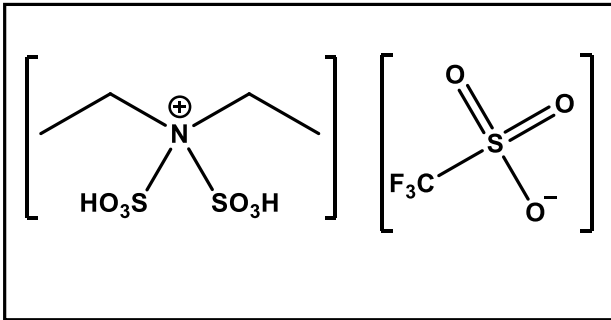
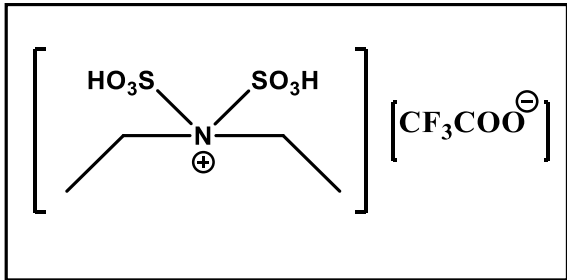
4.4.1 Synthesis of the N-SO₃H functionalized imidazolium and ammonium based ionic liquids

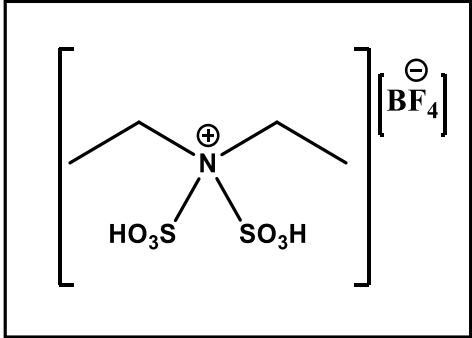
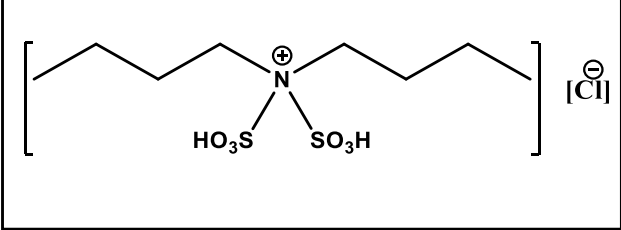
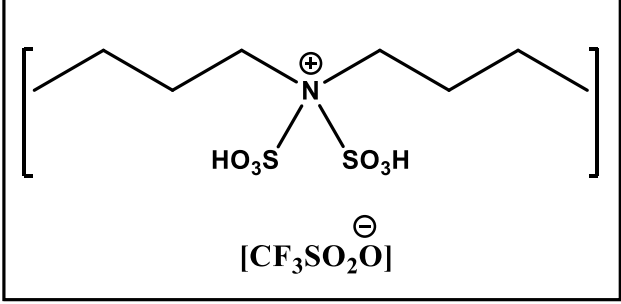
Three series of N-SO₃H functionalized ionic liquids of 2-ethyl-1,3-disulfoimidazolium [EDSIM], N,N-disulfodiethylammonium [DEDSA] and N,N-disulfodibutylammonium [DBDSA] cations with four different anions ($X^- = Cl^-, BF_4^-, CF_3COO^-$ and OTf^-) were prepared according to the reported procedure, which involved the formation of chloride ILs in 1st step [1, 14]. The first step involves dissolving 20 mmol of 2-ethylimidazole/diethylamine in dry CH₂Cl₂ (10 mL) in a 100 mL round bottomed flask with constant stirring. In case of dibutylamine (20 mmol), hexane was used in place of CH₂Cl₂ as a reaction medium. Chlorosulphonic acid (ClSO₃H) (40 mmol) was added then drop wise to the stirred solution of 2-ethylimidazole/diethylamine in CH₂Cl₂ or dibutylamine in hexane over a period of 3 minutes at ice-cold conditions to produce the respective chloride based ILs i.e. [EDSIM][Cl]/[DEDSA][Cl]/[DBDSA][Cl] [14]. It was then stirred at room temperature for 30 minutes. Evaporation of the solvent CH₂Cl₂ (or hexane) under reduced pressure yielded the light yellow/light brown coloured viscous chloride ILs.

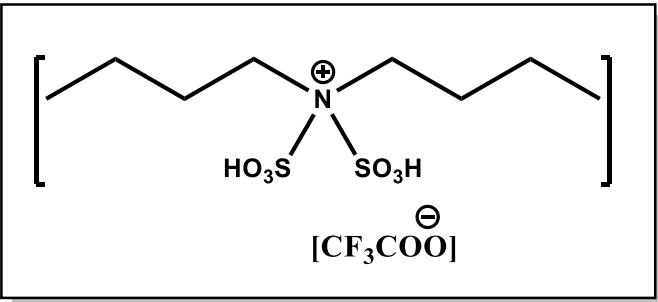
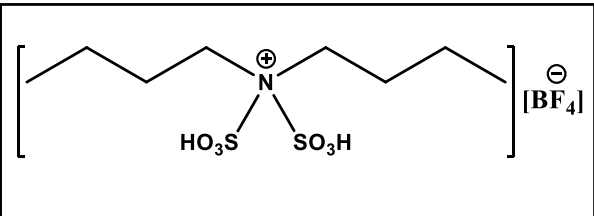
For synthesis of the CF₃COO⁻/CF₃SO₃⁻ anion containing ILs, 20 mmol of CF₃COOH/CF₃SO₃H was added to the crude chloride ILs of three organic cations and stirred at 80 °C for 2 hours to produce the corresponding anion exchanged trifluoroacetate/triflate ILs (**Scheme 4.1 A & B**) [14]. The HCl gas generated was removed through the outlet connected to a vacuum system over water and an alkali trap. The crude ILs were washed with dry CH₂Cl₂ (3 × 5 mL) because of their immiscibility in it and then decanted and dried in vacuum evaporator to get the analytically pure viscous/paste-like ionic liquids.

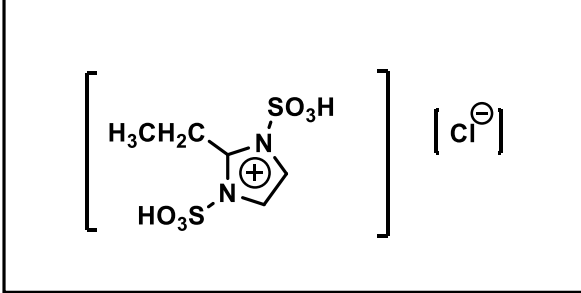
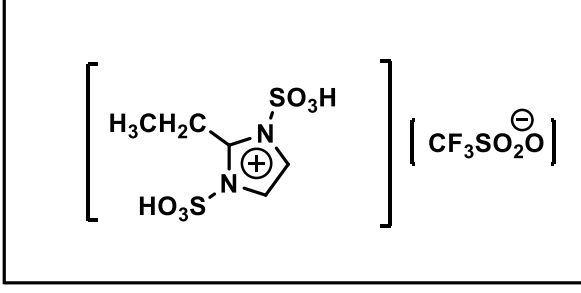
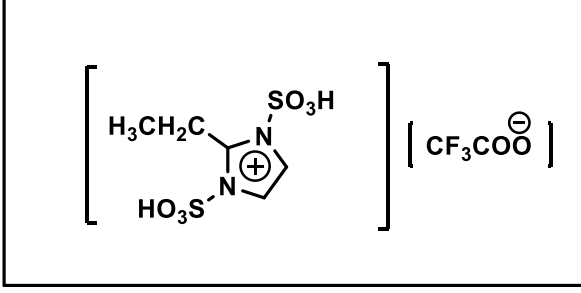
In case of the BF₄⁻ anion containing ILs, the respective chloride ILs (20 mmol) were treated with NaBF₄ (20 mmol) in 20 mL of acetonitrile for 72 hours (**Scheme 4.1 A & B**) at room temperature for the metathesis reaction. NaBr salt was precipitated out and was removed from the IL solution in acetonitrile by filtration. The evaporation of acetonitrile solution yielded [DEDSA][BF₄]/[EDSIM][BF₄]/[DBDSA][BF₄] as paste-like yellowish brown/yellowish green colored liquids.

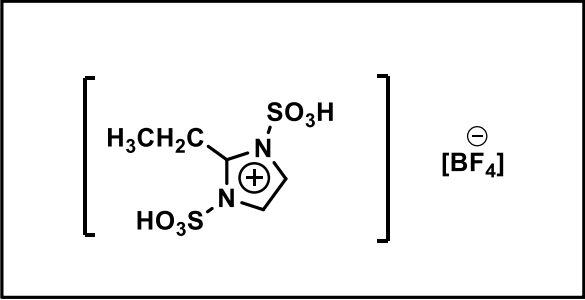
4.4.2 Spectral data of the BAILs

Sl. No.	Ionic liquid	Spectral data
1	 <p>N,N-Disulfodiethylammonium chloride [DEDSA][Cl]</p>	Light brown viscous liquid; FT-IR (KBr) cm^{-1} : 3423, 2920, 2849, 1635, 1460, 1125, 1049, 879, 775, 579; ^1H NMR (DMSO- d_6 , 400MHz): δ 8.34 (s, 2H), 2.85-2.80 (m, 4H), 1.10(t, $J = 8.0$ Hz, 6H); ^{13}C NMR (DMSO- d_6 , 100 MHz): δ 41.7, 11.7.
2	 <p>N,N-Disulfodiethylammonium trifluoromethanesulphonate [DEDSA][OTf]</p>	Dark brown gel; FT-IR (KBr) cm^{-1} : 3439, 2926, 2859, 1650, 1466, 1237, 1171, 1056, 1042, 880, 637, 588; ^1H NMR (DMSO- d_6 , 400 MHz): δ 8.15 (s, 2H), 2.85-2.81(m, 4H), 1.11-1.06(m, 6H); ^{13}C NMR (DMSO- d_6 , 100MHz): δ 123.1, 41.9, 11.3.
3	 <p>N,N-Disulfodiethylammonium trifluoroacetate [DEDSA][TFA]</p>	Brown viscous liquid; FT-IR (KBr) cm^{-1} : 3428, 2920, 2845, 1742, 1637, 1448, 1239, 1162, 1020, 884, 772 and 595; ^1H NMR (DMSO- d_6 , 400MHz): δ 8.21 (s, 2H), 2.85-2.80(m, 4H), 1.10 (t, $J = 8.0$ Hz, 6H) ; ^{13}C NMR (DMSO- d_6 , 100 MHz) : δ 159.1, 42.1, 11.6.

4	 <p>N,N-Disulfodiethylammonium tetrafluoroborate [DEDSA][BF₄]</p>	<p>Brownish yellow gel; FT-IR (KBr) cm⁻¹: 3442, 2930, 2852, 2505, 1661, 1486, 1390, 1108, 1021, 872, 778, 590; ¹H NMR (DMSO-d₆, 400 MHz) : δ 8.19 (s, 2H), 2.85 (s, 4H), 1.17-1.10 (m, 6H); ¹³C NMR (DMSO-d₆, 100 MHz): δ 41.97, 11.27; ¹⁹F NMR (DMSO-d₆, 376 MHz) : δ -148.28.</p>
5	 <p>N,N-Disulfodibutylammonium chloride [DBDSA][Cl]</p>	<p>Brown viscous liquid; FT-IR (KBr) cm⁻¹: 3429, 2959, 2923, 2855, 1627, 1467, 1238, 1165, 1047, 1019, 882, 874, 586; ¹H NMR (DMSO-d₆, 400 MHz) : δ 8.52 (s, 2H), 2.73 (s, 4H), 1.49-1.48 (m, 4H), 1.20-1.19 (s, 4H), 0.77 - 0.76 (m, 6H) ; ¹³C NMR (DMSO-d₆, 100 MHz): δ 47.2, 27.4, 19.9, 13.2.</p>
6	 <p>N,N-Disulfodibutylammonium trifluoromethanesulphonate [DBDSA][OTf]</p>	<p>Dark Brown gel; FT-IR (KBr) cm⁻¹: 3439, 2966, 2936, 2878, 1724, 1634, 1473, 1257, 1195, 1069, 1032, 880, 874, 774, 747, 640, 580, 512, 459; ¹H NMR (DMSO-d₆, 400 MHz) : δ 8.17 (s, 2H), 2.80-2.76 (m, 4H), 1.50-1.45 (m, 4H), 1.27-1.20 (m, 4H), 0.83-</p>

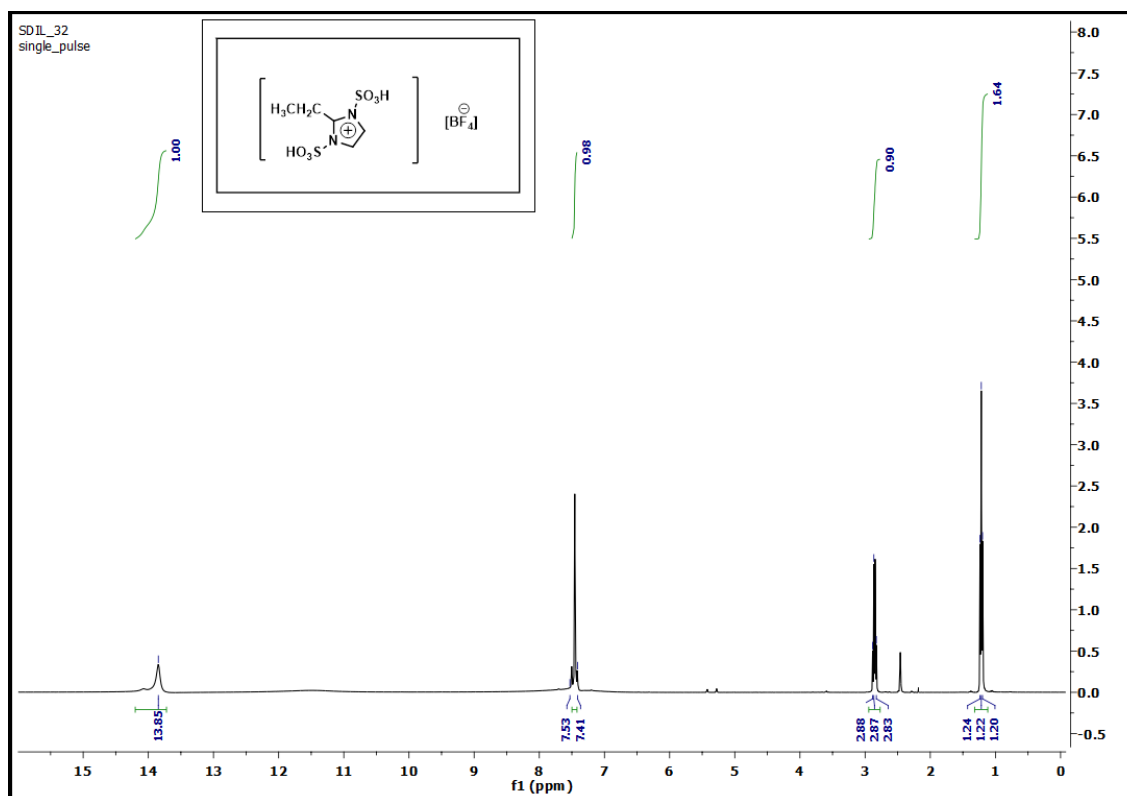
		0.76 (m, 6H); ^{13}C NMR (DMSO- d_6 , 100 MHz): δ 122.8, 46.6, 28.3, 19.6, 13.2.
7	 <p>N,N-Disulfodibutylammonium trifluoroacetate [DBDSA][TFA]</p>	Dark Brown Viscous liquid; FT-IR (KBr) cm^{-1} : 3429, 2966, 2930, 2878, 1789, 1634, 1454, 1294, 1232, 1163, 1072, 1019, 882, 847, 572, 451; ^1H NMR (DMSO- d_6 , 400 MHz) : δ 8.38 (s, 2H), 2.79 (s, 4H), 1.53-1.48 (m, 4H), 1.28-1.23 (m, 4H), 0.84-0.81 (m, 6H); ^{13}C NMR (DMSO- d_6 , 100 MHz): δ 159.6, 46.9, 27.9, 19.6, 12.8.
8	 <p>N,N-Disulfodibutylammonium tetrafluoroborate [DBDSA][BF$_4$]</p>	Light brown gel; FT-IR (KBr) cm^{-1} : 3432, 2969, 2930, 2872, 1726, 1662, 1485, 1375, 1185, 1053, 878, 584; ^1H NMR (DMSO- d_6 , 400 MHz) : δ 8.20 (s, 2H), 2.75 (s, 4H), 1.94-1.76 (m, 4H), 1.45-1.20 (m, 4H), 0.76 (s, 6H); ^{13}C NMR (DMSO- d_6 , 100 MHz): δ 46.9, 27.1, 19.6 and 13.6; ^{19}F NMR (DMSO- d_6 , 376 MHz) : δ -148.3.

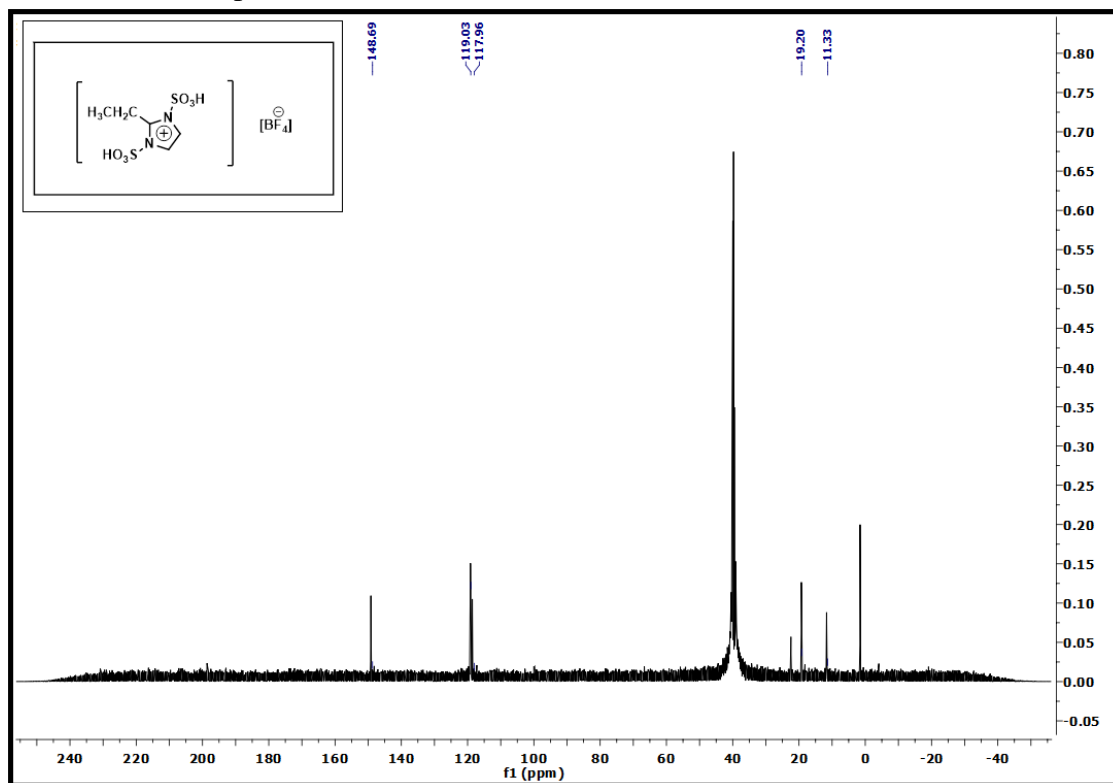
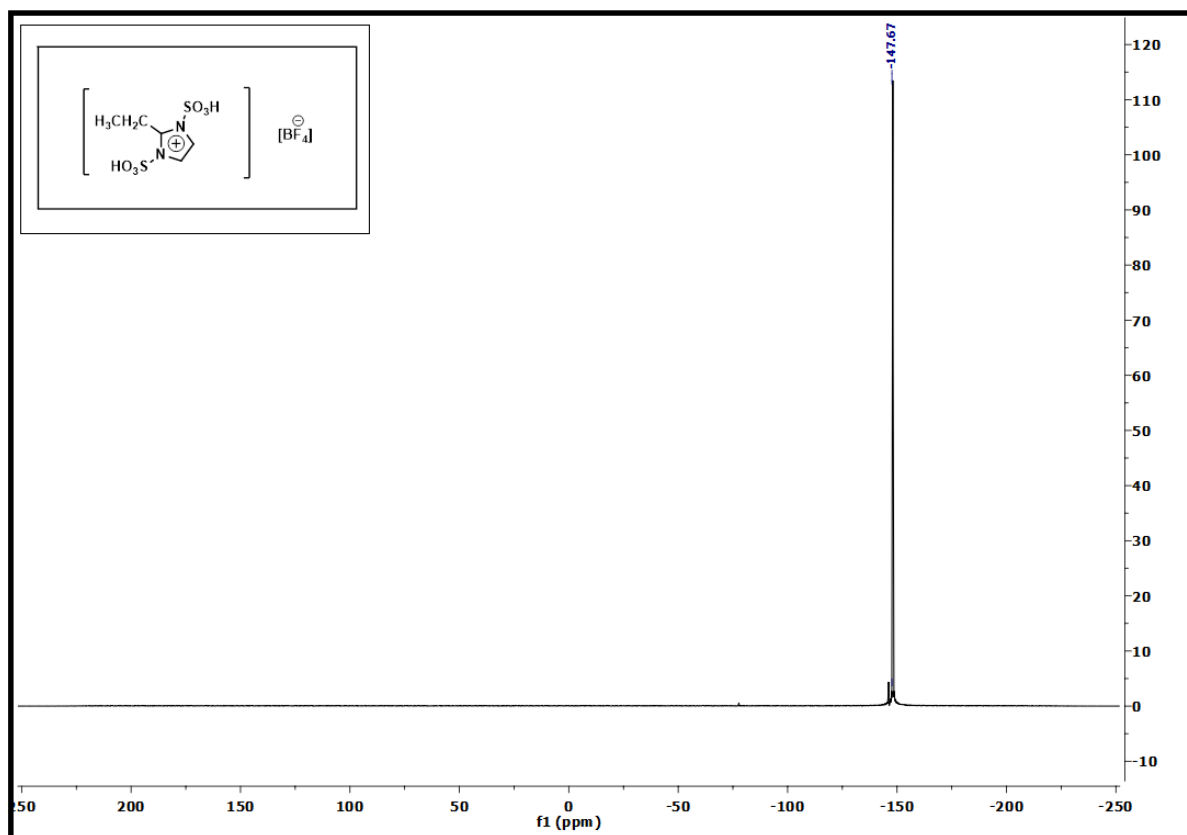
9	 <p style="text-align: center;">2-Ethyl-1,3-disulfoimidazolium chloride ([EDSIM][Cl])</p>	<p>Yellow viscous liquid; FT-IR (KBr) cm^{-1} : 3437, 2929, 2860, 1629, 1453, 1176, 1054, 872, 750, 581; ^1H NMR (DMSO-d_6, 400 MHz): δ 13.95 (s, 1H) 12.96 (s, 1H), 7.47-7.42 (m, 2H), 2.88-2.84 (m, 2H), 1.24-1.18 (m, 3H); ^{13}C NMR (DMSO-d_6, 100MHz): δ 149.3, 118.9, 18.8, 12.4.</p>
10	 <p style="text-align: center;">2-Ethyl-1,3-disulfoimidazolium trifluoromethanesulfonate ([EDSIM][OTf])</p>	<p>Brown gel; FT-IR (KBr) cm^{-1} : 3445, 2936, 2845, 1635, 1455, 1256, 1171, 1056, 1023, 869, 753, 631, 573; ^1H NMR (DMSO-d_6, 400 MHz): δ 13.90 (s, 2H), 7.39 (s, 2H), 2.83-2.75 (m, 2H), 1.20-1.15 (m, 3H); ^{13}C NMR (DMSO-d_6, 100 MHz): δ 148.7, 119.1, 116.4, 19.6, 11.3.</p>
11	 <p style="text-align: center;">2-Ethyl-1,3-disulfoimidazolium trifluoroacetate ([EDSIM][TFA])</p>	<p>Brown viscous liquid ; FT-IR (KBr) cm^{-1} : 3448, 2923, 2853, 1760, 1626, 1451, 1184, 1060, 884, 758, 698, 585; ^1H NMR (DMSO-d_6, 400 MHz) : δ 13.79 (s, 2H), 7.47 (s, 2H), 2.88 (q, $J = 8.0$ Hz, 2H), 1.22 (t, $J = 8.0$ Hz, 3H); ^{13}C NMR (DMSO-d_6, 100 MHz) : δ 159.2, 149.5, 119.4, 116.4, 19.6 , 10.9.</p>

12	<div style="text-align: center;">  <p>2-Ethyl-1,3-disulfoimidazolium tetrafluoroborate ([EDSIM][BF₄])</p> </div>	<p>Greenish yellow gel; FT-IR (KBr) cm^{-1} : 3451, 2923, 2845, 1635, 1481, 1262, 1146, 1030, 759, 586; ^1H NMR (DMSO-d_6, 400 MHz): δ 13.85 (s, 2H), 7.53-7.41 (m, 2H), 2.88-2.83 (m, 2H), 1.24-1.20 (m, 3H); ^{13}C NMR (DMSO-d_6, 100MHz) : δ 148.7, 119.0, 117.9, 19.2, 11.3; ^{19}F NMR (DMSO-d_6, 376 MHz) : -147.7.</p>
----	--	---

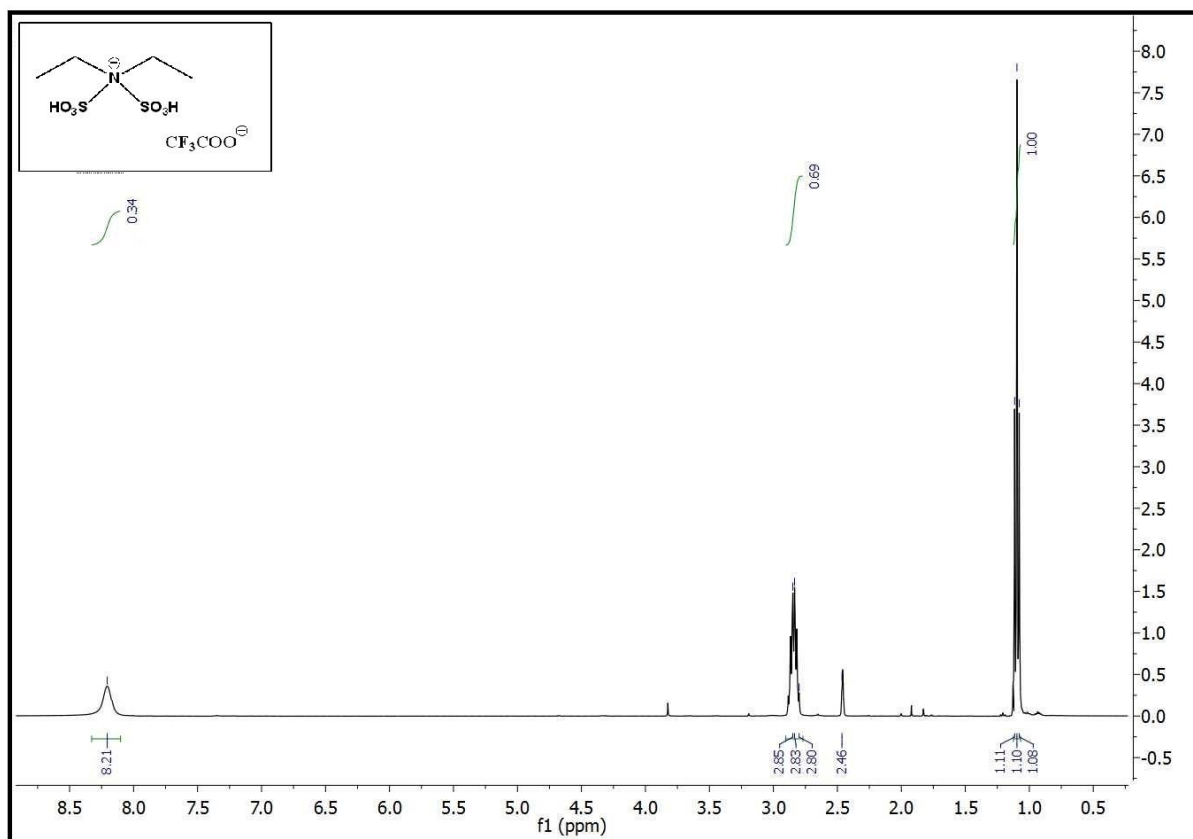
4.4.3 NMR spectra of the [EDSIM][BF₄] & [DBDSA][TFA] ionic liquids

1. ^1H NMR spectra of [EDSIM][BF₄]

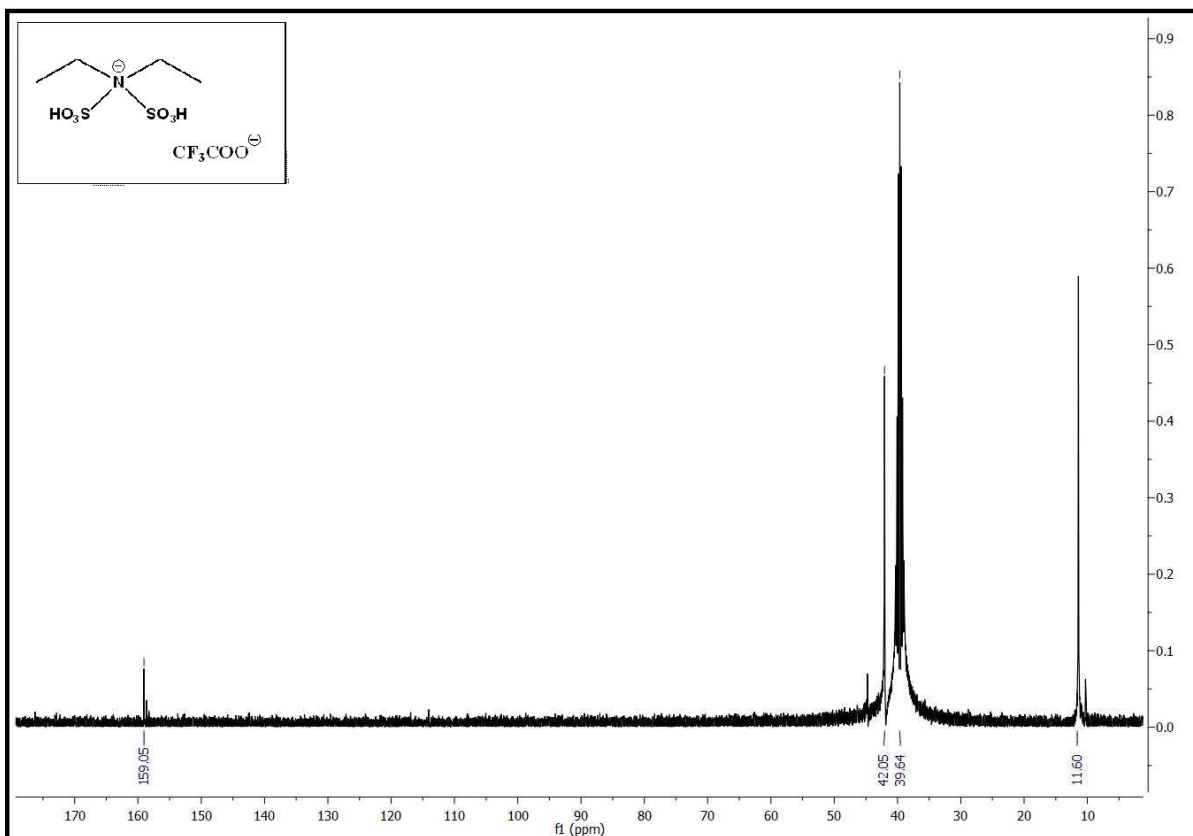


2. ^{13}C NMR spectra of [EDSIM][BF₄]3. ^{19}F NMR spectra of [EDSIM][BF₄]

4. ^1H NMR spectra of [DEDSA][TFA]



5. ^{13}C NMR spectra of [DEDSA][TFA]



Bibliography

- [1] Dutta, A. K., Gogoi, P., Saikia, S., and Borah, R. *N,N*-disulfo-1,1,3,3-tetramethylguanidinium carboxylate ionic liquids as reusable homogeneous catalysts for multicomponent synthesis of tetrahydrobenzo[*a*]xanthene and tetrahydrobenzo[*a*]acridine derivatives. *Journal of Molecular Liquids*, 225:585-591, 2017.
- [2] Kore, R. and Srivastava, R. Influence of $-SO_3H$ functionalization (N- SO_3H or NR- SO_3H , where R= alkyl/benzyl) on the activity of Brønsted acidic ionic liquids in the hydration reaction. *Tetrahedron Letters*, 53(26):3245-3249, 2012.
- [3] Xu, F., Sun, J., Konda, N. M., Shi, J., Dutta, T., Scown, C. D., Simmons, B. A., and Singh, S. Transforming biomass conversion with ionic liquids: process intensification and the development of a high-gravity, one-pot process for the production of cellulosic ethanol. *Energy & Environmental Science*, 9(3):1042-1049, 2016.
- [4] da Costa Lopes, A. M. and Bogel-Lukasik, R. Acidic ionic liquids as sustainable approach of cellulose and lignocellulosic biomass conversion without additional catalysts. *ChemSusChem*, 8(6):947-965, 2015.
- [5] Tiago, G. A., Matias, I. A., Ribeiro, A. P., and Martins, L. M. Application of ionic liquids in electrochemistry-Recent advances. *Molecules*, 25(24):5812, 2020.
- [6] Mallakpour, S. and Rafiee, Z. New developments in polymer science and technology using combination of ionic liquids and microwave irradiation. *Progress in Polymer Science*, 36(12):1754-1765, 2017.
- [7] Ho, T. D., Zhang, C., Hantao, L. W., and Anderson, J. L. Ionic liquids in analytical chemistry: fundamentals, advances, and perspectives. *Analytical Chemistry*, 86(1):262-285, 2014.
- [8] Arora, K., Shikha, P., Abdelbaky, R. M. K., and Kang, T. S. Modulation of morphological, optical and magnetic properties of Cr-doped $La_{0.9}Ce_{0.1}FeO_3$ nanoferrites synthesized by surface-active ionic liquid aided hydrothermal route. *Applied Physics A*, 127:1-9, 2021.
- [9] Leu, M., Campbell, P., and Mudring, A. V. Synthesis of luminescent semiconductor nanoparticles in ionic liquids—the importance of the ionic liquid in the formation of quantum dots. *Green Chemistry Letters and Reviews*, 14(1):128-136, 2021.

- [10] Muginova, S. V., Myasnikova, D. A., Kazarian, S. G., and Shekhovtsova, T. N. Applications of ionic liquids for the development of optical chemical sensors and biosensors. *Analytical Sciences*, 33(3):261-265, 2017.
- [11] Alexandre, M. and Nakamoto, T. Study of room temperature ionic liquids as gas sensing materials in quartz crystal microbalances. *Sensors*, 20(14):4026, 2020.
- [12] Al-Othman, A., Nancarrow, P., Tawalbeh, M., Ka'ki, A., El-Ahwal, K., El Taher, B., and Alkasrawi, M. Novel composite membrane based on zirconium phosphate-ionic liquids for high temperature PEM fuel cells. *International Journal of Hydrogen Energy*, 46(8):6100-6109, 2021.
- [13] Watanabe, M., Thomas, M. L., Zhang, S., Ueno, K., Yasuda, T., and Dokko, K. Application of ionic liquids to energy storage and conversion materials and devices. *Chemical Reviews*, 117(10):7190-7239, 2017.
- [14] Dutta, A. K., Gogoi, P., and Borah, R. Synthesis of dibenzoxanthene and acridine derivatives catalyzed by 1, 3-disulfonic acid imidazolium carboxylate ionic liquids. *RSC Advances*, 4(78):41287-41291, 2014.
- [15] Zolfigol, M. A., Khazaei, A., Moosavi-Zare, A. R., Zare, A., and Khakyzadeh, V. Rapid synthesis of 1-amidoalkyl-2-naphthols over sulfonic acid functionalized imidazolium salts. *Applied Catalysis A: General*, 400(1-2):70-81, 2011.
- [16] Boruń, A., Fernandez, C., and Bald, A. Conductance studies of aqueous ionic liquids solutions [emim][BF₄] and [bmim][BF₄] at temperatures from (283.15 to 318.15) K. *International Journal of Electrochemical Science*, 10(3):2120-2129, 2015.
- [17] Thawarkar, S., Khupse, N. D., and Kumar, A. Comparative investigation of the ionicity of aprotic and protic ionic liquids in molecular solvents by using conductometry and NMR spectroscopy. *ChemPhysChem*, 17(7):1006-1017, 2016.
- [18] O'Mahony, A. M., Silvester, D. S., Aldous, L., Hardacre, C., and Compton, R. G. Effect of water on the electrochemical window and potential limits of room-temperature ionic liquids. *Journal of Chemical & Engineering Data*, 53(12):2884-2891, 2008.
- [19] Chiappe, C. and Rajamani, S. Structural effects on the physico-chemical and catalytic properties of acidic ionic liquids: an overview. *European Journal of Organic Chemistry*, 2011(28):5517-5539, 2011.

- [20] Fernandes, A. M., Rocha, M. A., Freire, M. G., Marrucho, I. M., Coutinho, J. A., and Santos, L. M. Evaluation of cation– anion interaction strength in ionic liquids. *The Journal of Physical Chemistry B*, 115(14):4033-4041, 2011.
- [21] Amarasekara, A. S. and Owereh, O. S. Thermal properties of sulfonic acid group functionalized Brønsted acidic ionic liquids. *Journal of thermal analysis and calorimetry*, 103(3):1027-1030, 2011.
- [22] Stettner, T., Gehrke, S., Ray, P., Kirchner, B., and Balducci, A. Water in protic ionic liquids: properties and use of a new class of electrolytes for energy-storage devices. *ChemSusChem*, 12(16):3827-3836, 2019.
- [23] Dutta, A. K., Gogoi, P., and Borah, R. Triphenylsulfophosphonium chlorometallates as efficient heterogeneous catalysts for the three-component synthesis of 2,3-dihydro-1,2,3-trisubstituted-1H-naphth[1,2-*e*][1,3]oxazines. *Polyhedron*, 123:184-191, 2017.
- [24] Zolfigol, M. A., Khazaei, A., Moosavi-Zare, A. R., and Zare, A. Ionic liquid 3-methyl-1-sulfonic acid imidazolium chloride as a novel and highly efficient catalyst for the very rapid synthesis of bis (indolyl) methanes under solvent-free conditions. *Organic Preparations and Procedures International*, 42(1):95-102, 2010.
- [25] Zolfigol, M. A., Khazaei, A., Moosavi-Zare, A. R., and Zare, A. 3-Methyl-1-sulfonic acid imidazolium chloride as a new, efficient and recyclable catalyst and solvent for the preparation of N-sulfonyl imines at room temperature. *Journal of the Iranian Chemical Society*, 7:646-651, 2010.
- [26] Moosavi-Zare, A. R., Zolfigol, M. A., Zarei, M., Zare, A., and Khakyzadeh, V. Preparation, characterization and application of ionic liquid sulfonic acid functionalized pyridinium chloride as an efficient catalyst for the solvent-free synthesis of 12-aryl-8,9,10,12-tetrahydrobenzo[*a*]-xanthen-11-ones. *Journal of Molecular Liquids*, 186:63-69, 2013.
- [27] Akbari, J., Heydari, A., Reza Kalhor, H., and Kohan, S. A. Sulfonic acid functionalized ionic liquid in combinatorial approach, a recyclable and water tolerant-acidic catalyst for one-pot Friedlander quinoline synthesis. *Journal of Combinatorial Chemistry*, 12(1):137-140, 2010.
- [28] Sarma, P., Dutta, A. K., and Borah, R. Design and exploration of–SO₃H group functionalized brønsted acidic ionic liquids (BAILs) as task-specific catalytic

- systems for organic reactions: a review of literature. *Catalysis Surveys from Asia*, 21:70-93, 2017.
- [29] Yuan, W. L., Yang, X., He, L., Xue, Y., Qin, S., and Tao, G. H. Viscosity, conductivity, and electrochemical property of dicyanamide ionic liquids. *Frontiers in Chemistry*, 6:59, 2018.
- [30] Wu, F., Xiang, J., Chen, R., Li, L., Chen, J., and Chen, S. The Structure– Activity Relationship and Physicochemical Properties of Acetamide-Based Brønsted Acid Ionic Liquids. *The Journal of Physical Chemistry C*, 114(47):20007-20015, 2010.
- [31] Olivier-Bourbigou, H., Magna, L., and Morvan, D. Ionic liquids and catalysis: Recent progress from knowledge to applications. *Applied Catalysis A: General*, 373(1-2):1-56, 2010.
- [32] De Vos, N., Maton, C., and Stevens, C. V. Electrochemical stability of ionic liquids: general influences and degradation mechanisms. *ChemElectroChem*, 1(8):1258-1270, 2014.
- [33] Wu, T. Y., Su, S. G., Lin, Y. C., Wang, H. P., Lin, M. W., Gung, S. T., and Sun, I. W. Electrochemical and physicochemical properties of cyclic amine-based Brønsted acidic ionic liquids. *Electrochimica Acta*, 56(2):853-862, 2010.
- [34] Khodadadi-Moghaddam, M., Habibi-Yangjeh, A., and Gholami, M. R. Solvatochromic parameters for binary mixtures of an ionic liquid with various protic molecular solvents. *Monatshefte für Chemie-Chemical Monthly*, 140:329-334, 2009.
- [35] Buzzeo, M. C., Hardacre, C., and Compton, R. G. Extended electrochemical windows made accessible by room temperature ionic liquid/organic solvent electrolyte systems. *ChemPhysChem*, 7(1):176-180, 2006.
- [36] Boruń, A. and Bald, A. Ionic association and conductance of ionic liquids in dichloromethane at temperatures from 278.15 to 303.15 K. *Ionics*, 22:859-867, 2006.
- [37] Zhou, H., Chen, L., Wei, Z., Lu, Y., Peng, C., Zhang, B., Zhao, X., Wu, L., and Wang, Y. Effect of ionic composition on physicochemical properties of mono-ether functional ionic liquids. *Molecules*, 24(17):3112, 2019.
- [38] Bešter-Rogač, M., Hunger, J., Stoppa, A., and Buchner, R. Molar conductivities and association constants of 1-butyl-3-methylimidazolium chloride and 1-butyl-3-

- methylimidazolium tetrafluoroborate in methanol and DMSO. *Journal of Chemical & Engineering Data*, 55(5):1799-1803, 2010.
- [39] Bešter-Rogač, M., Hunger, J., Stoppa, A., and Buchner, R. 1-Ethyl-3-methylimidazolium ethylsulfate in water, acetonitrile, and dichloromethane: molar conductivities and association constants. *Journal of Chemical & Engineering Data*, 56(4):1261-1267, 2011.
- [40] Bešter-Rogač, M., Stoppa, A., and Buchner, R. Ion association of imidazolium ionic liquids in acetonitrile. *The Journal of Physical Chemistry B*, 118(5):1426-1435, 2014.
- [41] Borun, A. and Bald, A. Conductometric studies of 1-ethyl-3-methylimidazolium tetrafluoroborate and 1-butyl-3-methylimidazolium tetrafluoroborate in 1-propanol at temperatures from (283.15 to 318.15) K. *International Journal of Electrochemical Science*, 9(6):2790-2804, 2014.
- [42] Borun, A. and Bald, A. Conductometric studies of 1-ethyl-3-methylimidazolium tetrafluoroborate and 1-butyl-3-methylimidazolium tetrafluoroborate in N, N-dimethylformamide at temperatures from (283.15 to 318.15) K. *Journal of Chemical & Engineering Data*, 57(2):475-481, 2012.
- [43] Kalugin, O. N., Voroshylova, I. V., Riabchunova, A. V., Lukinova, E. V., and Chaban, V. V. Conductometric study of binary systems based on ionic liquids and acetonitrile in a wide concentration range. *Electrochimica Acta*, 105:188-199, 2013.
- [44] Voroshylova, I. V., Smaga, S. R., Lukinova, E. V., Chaban, V. V., and Kalugin, O. N. Conductivity and association of imidazolium and pyridinium based ionic liquids in methanol. *Journal of Molecular Liquids*, 203:7-15, 2015.
- [45] Seki, S., Kobayashi, T., Kobayashi, Y., Takei, K., Miyashiro, H., Hayamizu, K., Tsuzuki, S., Mitsugi, T., and Umebayashi, Y., Effects of cation and anion on physical properties of room-temperature ionic liquids. *Journal of Molecular Liquids*, 152(1-3):9-13, 2010.
- [46] Driessen, W. L., Reedijk, J., Dunbar, K. R., and Pence, L. E. Solid solvates: The use of weak ligands in coordination chemistry. In *Inorganic Syntheses*, pages 111-118, ISBN: 9780470132609. John Wiley & Sons, Inc., 1992.

- [47] Beck, W. and Suenkel, K. Metal complexes of weakly coordinating anions. Precursors of strong cationic organometallic Lewis acids. *Chemical Reviews*, 88(7):1405-1421, 1988.
- [48] Zhou, Z. B., Matsumoto, H., and Tatsumi, K. Low-melting, low-viscous, hydrophobic ionic liquids: aliphatic quaternary ammonium salts with perfluoroalkyltrifluoroborates. *Chemistry-A European Journal*, 11(2):752-766, 2005.
- [49] Fitchett, B. D., Knepp, T. N., and Conboy, J. C. 1-Alkyl-3-methylimidazolium bis (perfluoroalkylsulfonyl) imide water-immiscible ionic liquids: the effect of water on electrochemical and physical properties. *Journal of the Electrochemical Society*, 151(7):E219, 2004.
- [50] Montanino, M., Carewska, M., Alessandrini, F., Passerini, S., and Appetecchi, G. B. The role of the cation aliphatic side chain length in piperidinium bis (trifluoromethanesulfonyl) imide ionic liquids. *Electrochimica Acta*, 57:153-159, 2011.
- [51] Appetecchi, G. B., Montanino, M., Zane, D., Carewska, M., Alessandrini, F., and Passerini, S. Effect of the alkyl group on the synthesis and the electrochemical properties of N-alkyl-N-methyl-pyrrolidinium bis (trifluoromethanesulfonyl) imide ionic liquids. *Electrochimica Acta*, 54(4):1325-1332, 2009.
- [52] Matsumoto, H. Electrochemical windows of room-temperature ionic liquids. In Ohno, H., editor, *Electrochemical Aspects of Ionic Liquids*, ISBN: 9780471762515. John Wiley & Sons, Inc., 2005.
- [53] Yim, T., Choi, C. Y., Mun, J., Oh, S. M., and Kim, Y. G. Synthesis and properties of acyclic ammonium-based ionic liquids with allyl substituents as electrolytes. *Molecules*, 14(5):1840-1851, 2009.
- [54] Mancini, P. M. E., Adam, C. G., Fortunato, G. G., and Vottero, L. A comparison of nonspecific solvent scales. Degree of agreement of microscopic polarity values obtained by different measurement methods, *Arkivoc*, 2004(16): 266-280, 2007.
- [55] Hofmann, K., Schreiter, K., Seifert, A., Ruffer, T., Lang, H., and Spange, S. Solvatochromism and linear solvation energy relationship of diol- and proline-functionalized azo dyes using the Kamlet-Taft and Catalan solvent parameter sets. *New Journal of Chemistry*, 32(12):2180-2188, 2008.

-
- [56] Nordness, O. and Brennecke, J. F. Ion dissociation in ionic liquids and ionic liquid solutions. *Chemical Reviews*, 120(23):12873-12902, 2020.
- [57] Tokuda, H., Tsuzuki, S., Susan, M. A. B. H., Hayamizu, K., and Watanabe, M. How ionic are room-temperature ionic liquids? An indicator of the physicochemical properties. *The Journal of Physical Chemistry B*, 110(39):19593-19600, 2006.
- [58] Spange, S., Lungwitz, R., and Schade, A. Correlation of molecular structure and polarity of ionic liquids. *Journal of Molecular Liquids*, 192:137-143, 2014.
- [59] Bains, G. K., Kim, S. H., Sorin, E. J., and Narayanaswami, V. The extent of pyrene excimer fluorescence emission is a reflector of distance and flexibility: analysis of the segment linking the LDL receptor-binding and tetramerization domains of apolipoprotein E3. *Biochemistry*, 51(31):6207-6219, 2012.
- [60] Bonhôte, P., Dias, A. P., Armand, M., Papageorgiou, N., Kalyanasundaram, K., and Grätzel, M. Hydrophobic, highly conductive ambient-temperature molten salts. *Inorganic Chemistry*, 37(1):166-166, 1998.
- [61] Ye, C., Gray, V., Mårtensson, J., and Börjesson, K. Annihilation versus excimer formation by the triplet pair in triplet-triplet annihilation photon upconversion. *Journal of the American Chemical Society*, 141(24):9578-9584, 2019.
- [62] Tamai, Y., Ohkita, H., Shimada, J., Bente, H., Ito, S., Yamanaka, S., Hisada, K., Tani, K., Kubono, K., and Shinmyozu, T. Dynamical excimer formation in rigid carbazolophane via charge transfer state. *The Journal of Physical Chemistry A*, 117(33):7776-7785, 2013.
- [63] Deng, M., Schley, N. D., and Ung, G. Solvent-Dependent Sensitization of Ytterbium and Neodymium via an Intramolecular Excimer. *Inorganic Chemistry*, 57(24):15399-15405, 2018.
- [64] Losetty, V., Sivapragasam, M., and Wilfred, C. D. A. P. Recent advances and thermophysical properties of acetate-based protic ionic liquids. *Chemical Sciences Journal*, 7:128, 2016.
- [65] Greaves, T. L. and Drummond, C. J. Protic ionic liquids: properties and applications. *Chemical Reviews*, 108(1):206-237, 2008.